Science of the Total Environment 882 (2023) 163347

Contents lists available at ScienceDirect

Science of the Total Environment

journal homepage: www.elsevier.com/locate/scitotenv

Impacts of climate change on wind energy potential in Australasia and South-East Asia following the Shared Socioeconomic Pathways

A. Fournier [a], A. Martinez [b], G. Iglesias [b,c,*]

[a] MINES-Paristech, Rue Claude Daunesse, Sophia Antipolis 06904, France
[b] MaREI, Environmental Research Institute & School of Engineering, University College Cork, College Road, Cork, Ireland
[c] University of Plymouth, School of Engineering, Computing & Mathematics, Marine Building, Drake Circus, Plymouth PL4 8AA, United Kingdom

HIGHLIGHTS

- Multi-model ensemble to investigate evolution of wind resources up to 2100
- Using novel climate-change scenarios, Shared Socioeconomic Pathways (SSPs)
- More specifically, two scenarios, moderate (SSP2-4.5) and high emissions (SSP5-8.5)
- Greater changes in general in high-emissions scenario, except for seasonal variability
- Drastic changes (>150 %) projected for end of century in certain regions, e.g., Vietnam, Borneo.

GRAPHICAL ABSTRACT

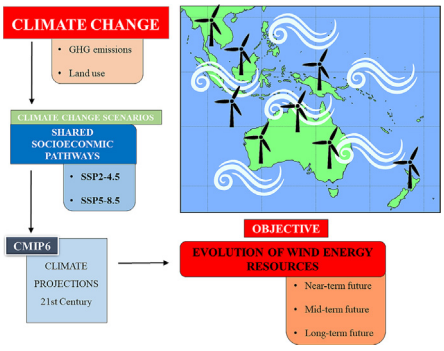

ARTICLE INFO

Editor: Pavlos Kassomenos

Keywords:
Wind power
Wind energy
Energy transition
Climate change
Shared Socioeconomic Pathways
Indochina

ABSTRACT

Wind energy is poised to play a major role in the energy transition. Fluctuations in global atmospheric circulation are expected as a result of climate change, and wind projections based on the most up-to-date scenarios of climate change, the Shared Socioeconomic Pathways (SSPs), anticipate significant changes in wind energy potential in many regions; so far, these changes have not been studied in Southeastern Asia and Australasia, a region with notable wind energy potential. This work investigates the evolution of wind power density and its temporal variability considering the latest scenarios of climate change, the SSPs. More specifically, two scenarios are considered, SSP2-4.5 and SSP5-8.5, corresponding to moderate and high emissions, respectively. As many as 18 global climate models are considered and compared against past-present data, and those that perform best are retained to build a large multi-model ensemble. The results show that projected changes in mean wind power density at the end of the 21st century are of little significance (typically below 5 %); nevertheless, this value can be far surpassed locally. In certain areas (e.g., Vietnam, Borneo) and seasons, remarkable changes in wind power density (exceeding 150 %) are anticipated. Typically, mean values and temporal variability changes are greater in the high-emissions scenario, however, seasonal variability is projected to be more pronounced in the moderate-emissions scenario. These effects of climate change on wind energy potential must be taken into account in the development of wind power in the region, for they will affect the energy production and, therefore, the economic viability of wind farms – not least in those areas where drastic changes are projected.

* Corresponding author at: MaREI, Environmental Research Institute & School of Engineering, University College Cork, College Road, Cork, Ireland.
E-mail address: gregorio.iglesias@ucc.ie (G. Iglesias).

http://dx.doi.org/10.1016/j.scitotenv.2023.163347
Received 13 January 2023; Received in revised form 29 March 2023; Accepted 3 April 2023
Available online 19 April 2023

1. Introduction

Through greenhouse gases (GHG) emissions, human influence has caused unprecedented changes in the global climate (IPCC, 2021). To limit this phenomenon it is necessary to cut carbon emissions; therefore, switching to low-carbon, renewable energy sources is critical. Wind power has the potential to play an important role in the energy transition; however, even though wind energy is an important tool for combating climate change, it is also very dependent on the climate itself. Although the available wind energy potential depends on different parameters (Foley et al., 2010), e.g., air density (Ulazia et al., 2019), it is particularly sensitive to variations in wind speeds - being proportional to the wind speed cubed, small fluctuations lead to more significant changes in wind power. Hence, evaluating future changes in wind energy potential is essential to manage upcoming investments (Foley et al., 2012), and climate change is the main driver of fluctuations in wind energy potential and storm surges (Pavlova et al., 2022). Studying the impact of climate change on the wind energy potential is crucial for the development of new wind energy installations and management of those in operation.

The goal of this work is to study the impact of climate change on wind energy potential in the region spanning from South-East Asia to Australia and New Zealand. The projected changes in wind power density in three different time horizons (near-, mid- and long-term future) in the 21st century based on two different climate change scenarios are computed and analysed. In this manner, it is evaluated whether areas previously overlooked may become the object of new wind energy installations, or if regions with an already well-developed wind energy industry may see their wind energy potential endangered or, conversely, be able to produce more energy. In any case, studying the evolution of wind energy potential is fundamental for the planning of future wind energy.

The prime drivers of wind climate in the area of study are the prevailing winds, which mostly depend on the latitude. The northernmost section of the region of study is affected by the trade winds, which are approximately located between 30°N and 10°N, affecting most of mainland South-East Asia and parts of the Philippines (Wind systems, 2021). Centred on the Equator, between 10°N and 10°S, is an area of low pressure with very calm prevailing winds both over land and ocean: the Intertropical Convergence Zone (ITCZ). South of the ITCZ is another area where the prevailing winds are Trade Winds, but contrarily to the northeasterly winds from the Northern Hemisphere they are southeasterly winds in the Southern Hemisphere, once again blowing towards the Equator. Around 30°S is another convergence area with rather calm winds: the subtropical highs or "horse" latitudes. Finally, in the southernmost part of the area of study is the area dominated by the Westerlies: particularly strong winds blowing from the West (Wind systems, 2021).

Several wind farms already exist within the area of study (Renewables, 2020). Australia accounts for the biggest total wind power capacity, with 10.2 GW. Other countries in the region of study also present several installations: Thailand (1.5 GW), New Zealand (513 MW) (Energy in new zealand, 2021), Vietnam (513 MW), the Philippines (427 MW) and Indonesia (154 MW) (Lee et al., 2021). Nonetheless, wind energy is rapidly growing as a result of the cutting of greenhouse gases emissions (Erdiwansyah et al., 2019), following the Paris agreement (United Nations, n.d.) and the emergence of new technological solutions such as offshore wind (López et al., 2018), which consists of wind turbines that may be mounted on monopiles (Perez-Collazo et al., 2019), jacket structures (Perez-Collazo et al., 2018) or floating platforms (Jonkman and Matha, 2010). Particularly, offshore wind is experiencing an important development in recent years - worldwide, 6.1 GW of newly installed capacity was commissioned in 2020 (G. Global Wind Energy Council, 2021) and a record of 21.1 GW in 2021 (G. Global Wind Energy Council, 2022). Following this development of the industry, the potential of the offshore wind energy potential has been widely explored in recent years, e.g., in the Western Mediterranean (Ulazia et al., 2017), the Iberian northern coastline (Ulazia et al., 2016), Thailand (Chancham et al., 2017). Furthermore, the focus has also been put on the study of the economic viability of offshore wind projects in different areas (Martinez and Iglesias, 2021a), e.g., the Mediterranean (Staschus et al., 2020), Atlantic Europe (Martinez and Iglesias, 2022a), the UK (Cavazzi and Dutton, 2016) or Ireland (Martinez and Iglesias, 2022b).

Importantly for this work, offshore energies, especially wind (Château et al., 2012; Pınarbaşı et al., 2019; Stelzenmüller et al., 2021) and wave (Bergillos et al., 2019; Martinez and Iglesias, 2020; Rodriguez-Delgado et al., 2018), have proven to be of special importance in small islands (Veigas et al., 2014), which abound in the study area. This aspect has been explored for the islands of Tenerife (Veigas and Iglesias, 2013), Crete (Lavidas and Venugopal, 2018), Fuerteventura (Veigas and Iglesias, 2014) or Naxos (Fyrippis et al., 2010). Furthermore, this technology represents a unique opportunity for combined exploitation (Ramos et al., 2022), e.g., wave-wind (Astariz et al., 2015) or wind-solar PV (López et al., 2020), and the possibility of hydrogen production (Dinh et al., 2021). It is apparent that the scope of wind energy is widening and additional areas may become the object of new wind installations; hence, studying the future wind energy potential is of utmost importance.

The anticipation of future climatic changes is often studied in literature by means of climate models (Arif et al., 2022). The impact of climate change on sea-surface winds in South-East Asia was previously studied (Herrmann et al., 2020) using data from a single global climate model (GCM) involved in the 5th phase of the Coupled Model Intercomparison Project (CMIP5), which considered the Representative Concentration Pathways (RCPs) scenarios for climate change (Taylor et al., 2012), introduced by the Intergovernmental Panel on Climate Change (ICPP) on its fifth Assessment Report (AR5) (Liao and Chang, 2014). In another study, the global evolution of wind speed, including both onshore and offshore regions with depths below 200 m, was studied using 12 GCMs from CMIP5 (Jung and Schindler, 2019) in RCP8.5. Importantly, these studies showed no significant changes in the wind energy potential in South Eastern Asia or Australasia.

With the 6th phase of the Coupled Model Intercomparison Project (CMIP6) (Eyring et al., 2016), data from a large number of GCMs were published considering the most complex and updated scenarios of future greenhouse gases emissions and land use, the Shared Socioeconomic Pathways (SSPs) (Riahi et al., 2017), introduced by the ICPP on its sixth Assessment Report (AR6) (IPCC, 2021). While previous scenarios (RCPs) described different levels of GHG emissions leading to certain radiative forcing, the more complex SSPs set the socioeconomic narratives (global population, growth of the economy, energy use, etc.) that have an impact on GHG emissions and land use, influencing the carbon cycle and thus the global climate. Other efforts were put into considering future trajectories of population, economic growth and greenhouse gas emissions in climate change scenarios, such as the SRES scenarios (Van Vuuren and O'Neill, 2006). However, these became dated and failed to reproduce large societal and global economic changes in the last years. Data from the CMIP6 have been successfully used to assess the impact of climate change on surface wind speed and wind power density in China (Wu et al., 2020), offshore China (Zhang and Li, 2021), the UK (Moradian et al., 2022a), North America (Martinez and Iglesias, 2022c), the Northwestern Passage (Qian and Zhang, 2020), Europe (Martinez and Iglesias, 2021b) and offshore Northern Europe (Martinez et al., 2023). Importantly, these studies showed that wind projections with the SSPs scenarios anticipate more pronounced changes in wind patterns than the previous scenarios. In Europe, an overall 15 % decrease in wind power density was predicted in the long-term future (Martinez and Iglesias, 2021b), and in North America, remarkable increases and decreases (over 100 % and 50 %, respectively) were predicted in specific regions (Martinez and Iglesias, 2022c). It is clear that these changes would be of great relevance for the wind energy industry, however, the SSPs have not been previously considered to study the evolution of wind energy potential in South-Eastern Asia and Australasia, and therein lies the motivation of this work. While previous studies showed no significant changes in the wind energy potential, wind projections with the SSPs may anticipate a more substantial evolution that could be of interest to the industry.

Other interesting aspects that ought to be considered are the general and intra-annual variability. A larger variability of the resource may have an important impact on project financing, as investors often prefer steadier revenues. Nonetheless, the evolution of the general and intra-annual variability is seldom studied. This is due to the fact that wind climate projections often lack sufficient temporal resolution to serve as the basis for statistically relevant studies - previous wind climate projections often provide monthly-averaged data. The GCMs involved in the CMIP6, however, provide daily-averaged wind climate projections.

This work considers for the first time the latest and most complex scenarios of climate change, the Shared Socioeconomic Pathways (SSPs), to assess the future of wind energy potential in South East Asia and Australasia. Projections on wind data from GCMs participating in the CMIP6 are considered, and those which are found to best reproduce past-present wind conditions are chosen to construct a multi-model ensemble (Yazdandoost et al., 2020). The impacts of climate change on the available wind energy potential are studied in the near-, mid- and long-term future by comparison with past-present data. Furthermore, daily data on wind speed are employed to study the evolution of the general and intra-annual variability.

The structure of the paper is as follows. In Section 2, the materials and methods employed in this work are described. Section 3 presents the results obtained in the research, with a discussion of key observations. Finally, in Section 4, conclusions are drawn.

2. Methodology

The area of study is defined by the following ranges of longitude and latitude: 48°S - 24°N and 90°E - 174°W respectively, as it is represented in Fig. 1. It includes most of South-East Asia, Papua New Guinea, Australia, New Zealand and a large number of island nations.

The climate change scenarios considered in the present work are two SSPs, specifically: SSP5-8.5, corresponding to a high-emission scenario, and SSP2-4.5, corresponding to a business-as-usual scenario with moderate emissions (Riahi et al., 2017). These scenarios are used as input for global climate models to produce projections on several climate variables, including surface wind speed. The models considered in this study are all involved in the CMIP6 activities (Eyring et al., 2016), the CMIP being a common framework for climate scientists to analyse, validate and improve climate model performances and to distribute their output data. All the GCMs involved in the CMIP6 activities providing projections on daily wind speed data using both scenarios of climate change are considered in this work (Table 1) (GCMs providing finer temporal resolution are also considered, in that case, mean daily wind data is calculated). Since the different models use various spatial resolutions, the data are remapped to a regular 1.5° × 1.5° (~104 km × ~104 km at zero degrees latitude) grid using a first-order conservative remapping, which maintains the flux integrals (Jones, 1999).

In order to validate the models and select those to be used in this study, their output values for the 2005–2014 period are compared to the ERA-5

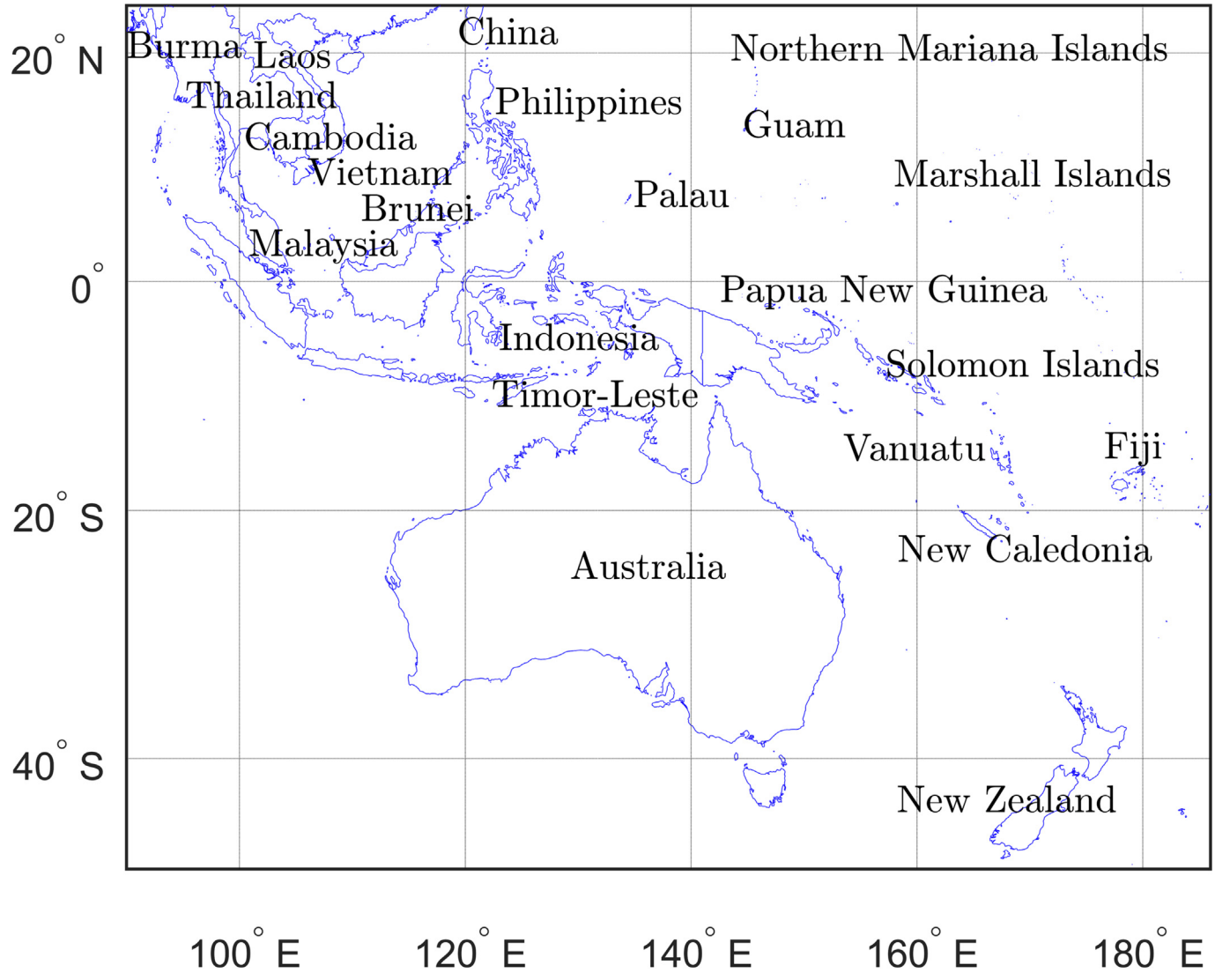

Fig. 1. Map of the area of study and relevant countries for the scale of the project.

Table 1
Global climate models considered in this work. The approximate resolution expressed in km is indicated at zero degrees latitude.

Model	Resolution	Ref
AWI-CM-1-1-MR	0.9375° × 0.9375° (~104 km × ~104 km)	(Semmler et al., 2019)
BCC-CSM2-MR	1.12° × 1.125° (~125 km × ~125 km)	(Xin et al., 2019)
FGOALS-f3-L	1° × 1.25° (~111 km × ~139 km)	(Yu, 2019)
CanESM5	1.775° × 2.1825° (~198 km × ~243 km)	(Swart et al., 2019)
ACCESS-CM2	1.25° × 1.875° (~139 km × ~209 km)	(Dix et al., 2019a; Dix et al., 2019b)
MPI-ESM1-2-HR	0.93° × 0.9375° (~104 km × ~104 km)	(Schupfner et al., 2019)
MPI-ESM1-2-LR	1.85° × 1.875° (~206 km × ~209 km)	(Wieners et al., 2019a; Wieners et al., 2019b)
EC-Earth3	0.7° × 0.7031° (~78 km × ~78 km)	(EC-Earth Consortium (EC-Earth), 2019)
INM-CM4-8	1.5° × 2° (~167 km × ~223 km)	(Volodin et al., 2019a; Volodin et al., 2019b)
INM-CM5-0	1.5° × 2° (~167 km × ~223 km)	(Volodin et al., 2019c; Volodin et al., 2019d)
IPSL-CM6A-LR	1.2676° × 2.5° (~141 km × ~278 km)	(Boucher et al., 2019)
MIROC6	1.4° × 1.4063° (~156 km × ~157 km)	(Shiogama et al., 2019)
MRI-ESM2-0	1.12° × 1.125° (~125 km × ~125 km)	(Yukimoto et al., 2019)
CESM2-WACCM	0.9424° × 1.25° (~105 km × ~139 km)	(Danabasoglu, 2019)
NorESM2-MM	0.9424° × 1.25° (~105 km × ~139 km)	(Bentsen et al., 2019)
KACE-1-0-G	1.25° × 1.875° (~139 km × ~209 km)	(Byun et al., 2019)
GFDL-CM4	1° × 1.25° (~111 km × ~139 km)	(Guo et al., 2018)
GFDL-ESM4	1° × 1.25° (~111 km × ~139 km)	(John et al., 2018)

Table 2
Percentage of statistically similar grid points for each climate model.

Model	Statistically similar grid points
IPSL-CM6A-LR	43 %
NorESM2-MM	43 %
CESM2-WACCM	42 %
GFDL-CM4	42 %
EC-Earth3	41 %
GFDL-ESM4	41 %
ACCESS-CM2	41 %
MIROC6	40 %
BCC-CSM2-MR	38 %
MPI-ESMI1-2-HR	38 %
FGOALS-f3-L	37 %
INM-CM5-0	37 %
INM-CM4-8	37 %
AWI-CM-1-1-MR	36 %
MRI-ESM2-0	36 %
KACE-1-0-G	36 %
CanESM5	36 %
MPI-ESM1-2-LR	20 %

reanalysis database from the European Centre for Medium-Range Weather Forecasts (ECMWF). The ERA-5 is the most recognized database for model validation (Hersbach and Dee, 2016), it has been extensively used for validating wind projections (Dosio et al., 2015; Carvalho et al., 2017; Bloom et al., 2008) and is the official dataset for validation in the CMIP downscaling projects (Gutowski et al., 2016). However, the ERA-5 is not without errors itself. Reportedly, although of generally acceptable performance, the limited resolution of the model may lead to over- and under-predictions of the wind resource in areas with high variations in topography – e.g., some under-predictions were found at a forested site in Wallaby Creek (Australia) (Gualtieri, 2021). The wind speed distributions from the individual models are compared with the ERA-5 database through a Kolmogorov-Smirnov (K-S) test, which determines whether two samples belong to the same distribution or not by comparing the absolute value of the maximum difference between their cumulative distributions with a critical value based on a significance level (Guthrie, 2020). First, the wind speed time series are centred so they have zero mean, in order to obtain a higher level of precision of the K-S test (Brands et al., 2013). Second, the two-sample K-S test is applied to the centred time series of each GCM against the centred time series of the ERA-5 database over the same time period (2005–2014) with a significance level of 5 %. The performance of the GCMs is measured as the number of grid points that have statistically

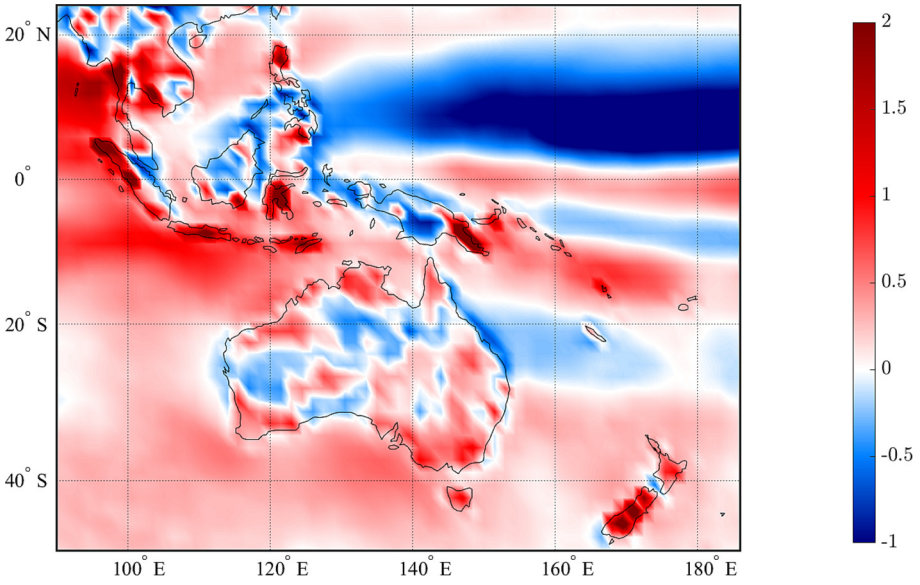

Fig. 2. Normalised bias of the multi-model ensemble historical (2005–2014) wind speed against the ERA-5 historical database.

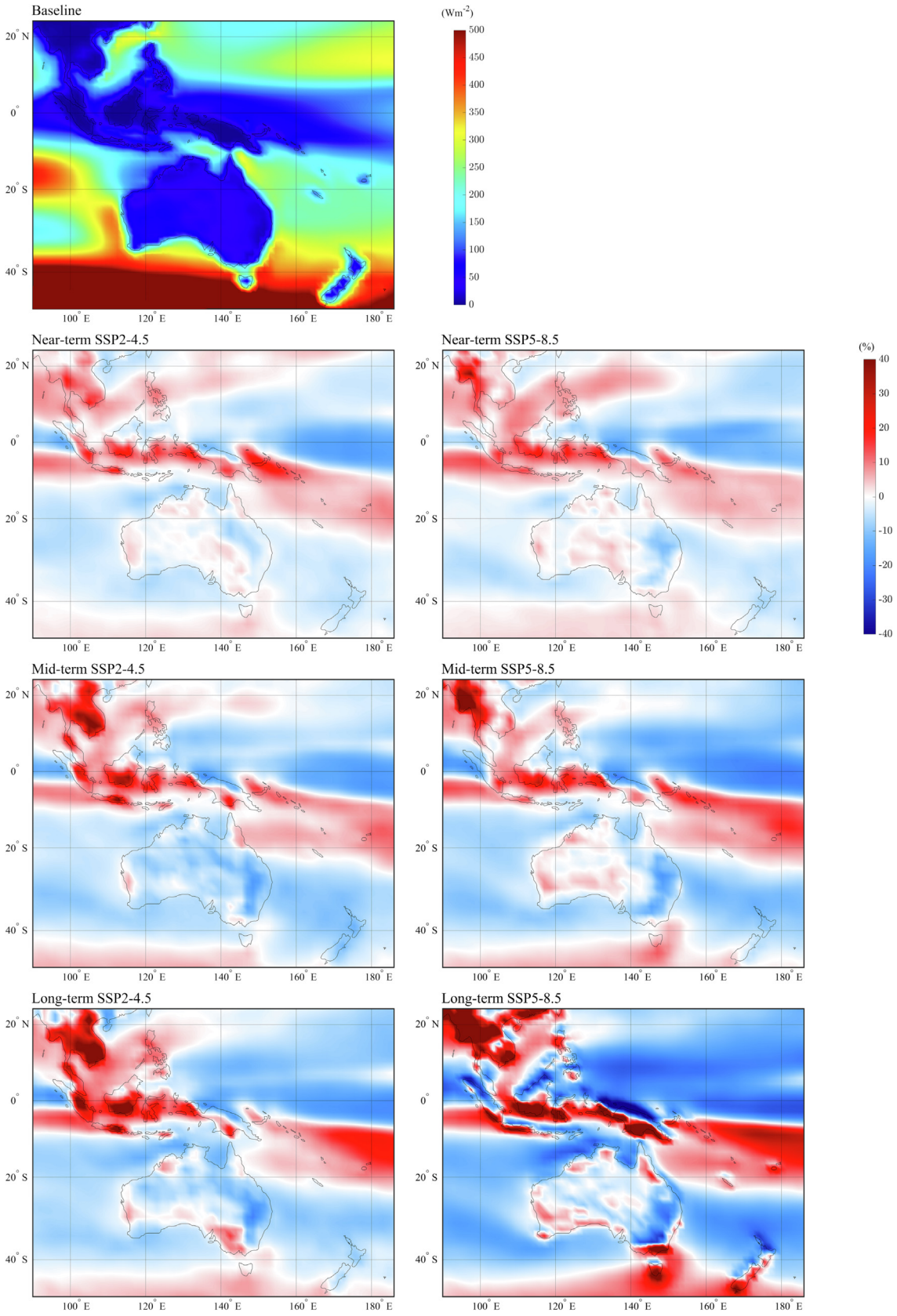

Fig. 3. Baseline values (Wm^{-2}) (uppermost panel) and near-, mid- and long-term evolution (%) of the mean wind power density for SSP2-4.5 (left) and SSP5-8.5 (right) climate change scenarios.

similar wind distributions to their ERA-5 counterpart, shown in Table 2 as a percentage of the total number of grid points.

The four models with >42 % statistically similar points are retained for the rest of this study, namely: IPSL-CM6A-LR, NorESM2-MM, CESM2-WACCM and GFDL-CM4. Data from these GCMs are used to build a Multi-Model Ensemble (MME) (Moradian et al., 2022b) following an unweighted approach (Pierce et al., 2009). By reducing individual uncertainties, results at a higher level of precision can be obtained (Tebaldi and Knutti, 2007). Wind speeds of the resulting MME are compared against the ERA-5 database via the normalised bias (θ):

$$\theta = \frac{U_{MME} - U_{ERA-5}}{\sigma_{ERA-5}}, \quad (1)$$

where U_{MME} and U_{ERA-5} are the wind speed values from the MME and ERA-5 database, respectively, and σ_{ERA-5} is the standard deviation of the ERA-5 database (Brands et al., 2013). The normalised bias is thus calculated at each grid point (Fig. 2).

Overall, the MME is in good agreement with the ERA-5 database, especially over large areas of open water, with the exception of a significant region in the Pacific Ocean between 0° and 20°N. Some discrepancies can be observed in regions such as Malaysia, New Guinea or South Island in New Zealand, which may be due to the relatively coarse resolution or the models. As a result, the features of coastal and mountainous areas, which may influence near-surface winds, cannot be fully taken into account.

In this work, the wind energy potential is quantified by the wind power density (P), a measure of the available wind energy at a certain location (in Wm^{-2}), and it is calculated as:

$$P = \frac{1}{2}\rho_{air}U^3, \quad (2)$$

where U is the wind speed and $\rho_{air} = 1.225\ \text{kgm}^{-3}$ is the air density.

The evolution of the wind energy potential is studied in three time periods: near-term future (2022–2031), mid-term future (2056–2065) and long-term future (2091–2100). For each period, data on the projected wind power density from the MME for both scenarios of climate change are used to calculate changes relative to the historical period (2005–2014) of the MME, hereinafter referred to as the baseline.

3. Results and discussion

Using the data and methods presented in the previous section, projections on wind power density of the multi-model ensemble are obtained. The evolution of mean wind power density, the general variability and the intra-annual variability is studied.

3.1. Mean wind power

The mean wind power density values are computed for the near-term, mid-term and long-term future and compared with the baseline (Fig. 3).

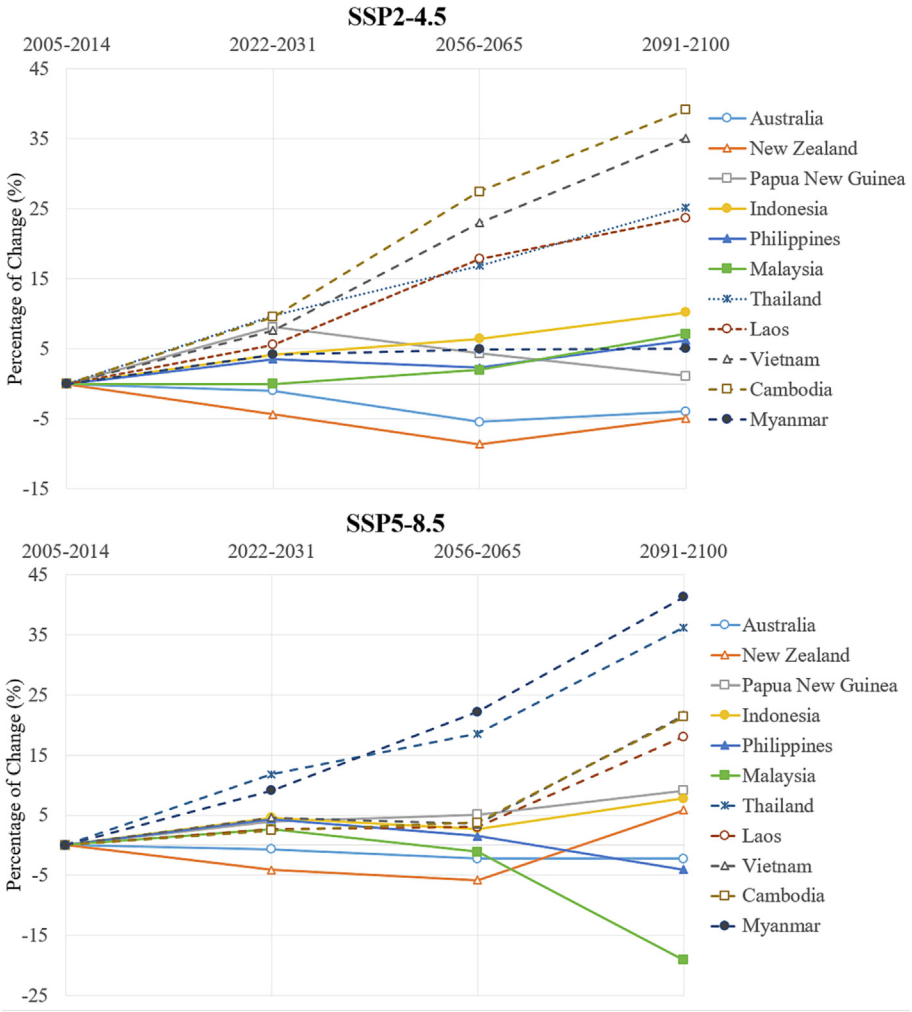

Fig. 4. Evolution (%) of mean wind power density in the near- (2022–2031), mid- (2056–2065) and long-term (2091–2100) future for SSP2-4.5 (upper panel) and SSP5-8.5 (lower panel) climate change scenarios.

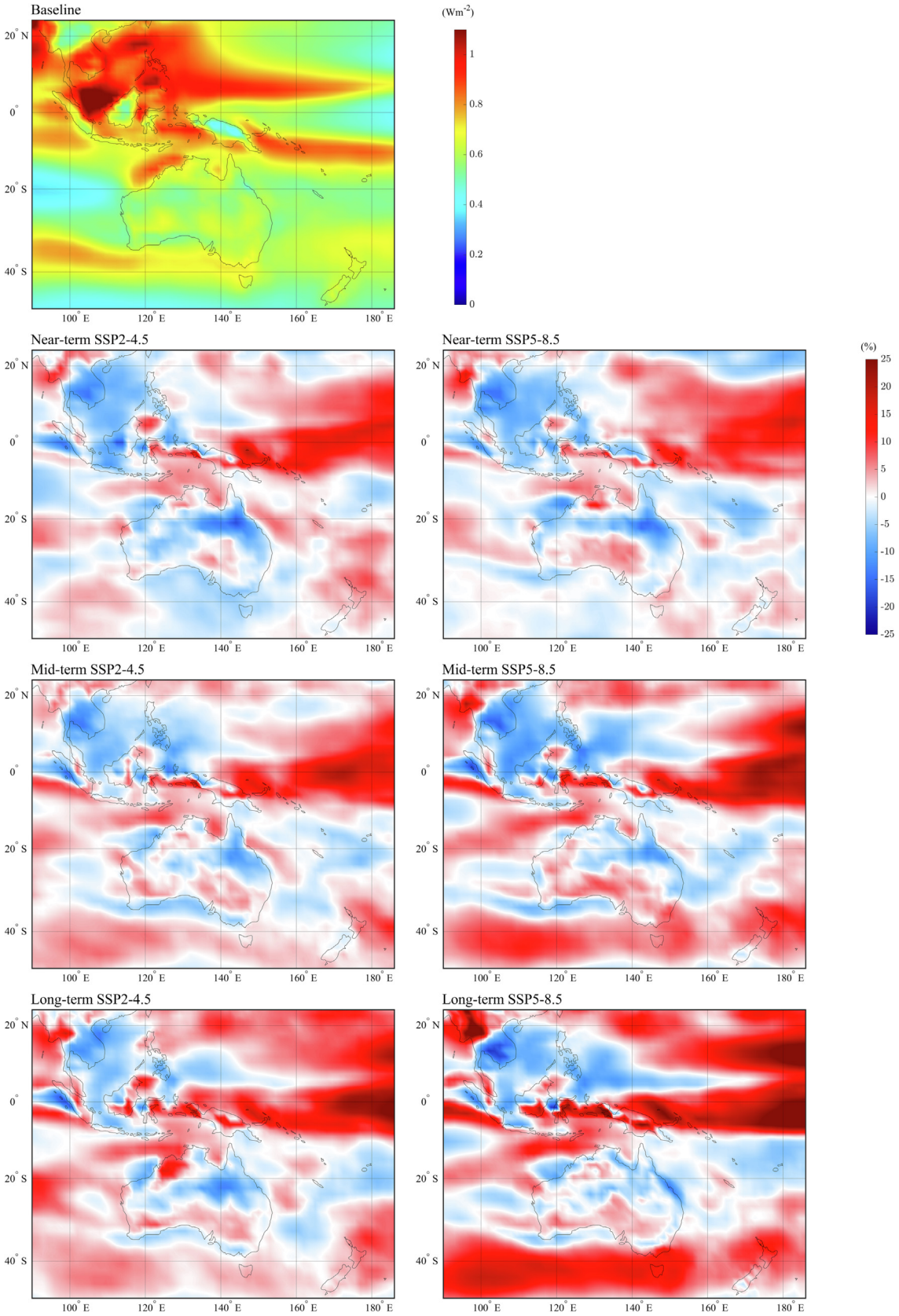

Fig. 5. Baseline values (uppermost panel) and near-, mid- and long-term evolution (%) of coefficient of variation for SSP2-4.5 (left) and SSP5-8.5 (right) climate change scenarios.

The area with the highest wind power density is located below 40°S, with values over 1100 Wm^{-2} provided by the Westerlies affecting Tasmania and parts of New Zealand. Significant wind power densities can also be found in the Indian Ocean off the western coast of Australia, around 400 Wm^{-2}, in the Coral Sea near the Cape York Peninsula, the Great Australian Bight and the South China Sea, with values reaching 300 Wm^{-2}.

In the near-term future, changes in wind power density relative to the baseline are between −20 % and +20 % in the SSP2-4.5 scenario, and between −20 % and +40 % in SSP5-8.5. These values can hardly be dismissed, especially taking into account the proximity between the near-term future (2022–2031) and the baseline (2005–2014).

In the mid-term (2056–2065) and long-term future (2091–2100), the differences with the baseline are significantly greater, reaching localised changes of up to +70 % in the SSP2-4.5 scenario and +150 % in the SSP5-8.5 scenario.

Despite these significant local changes, the average overall changes in the long-term future are limited in large areas of the region, e.g., Australia, of the order of −1.5 % in the SSP2-4.5 scenario and −3.5 % in the SSP5-8.5 scenario. This is the reason large countries, e.g., Australia, show small variations in the projected wind energy resource, while smaller countries may be the focus of important, concentrated changes, e.g., Cambodia (Fig. 4). General trends over the whole area of study cannot be discerned, and the evolution of the wind energy potential strongly varies on a regional level. This can be explained by the fact that the study area is large and, therefore, includes diverse climate zones, which will experience different wind pattern evolution. An example of this phenomenon is Australia, where a limited long-term decrease in wind power density (of approximately −4 %) is forecasted in both scenarios, while various regions scattered around the country experience notable wind power density increases, especially in the SSP5-8.5 scenario (up to +50 % locally).

The case of Australia is especially interesting since it consists of a large landmass where little changes are anticipated overall - in contrast with another large landmass, Europe, where significant changes are anticipated (Martinez and Iglesias, 2021b). On the contrary, an area with considerable changes is Southern Borneo - in the SSP2-4.5 scenario, a notable increase of up to 60 % in wind power density, and in the SSP5-8.5 scenario, an exceptional growth of 150 %. The northern part of the island, conversely, experiences much more limited changes.

Overall, both climate change scenarios agree on the general trends of wind power density evolution. The scenario with the highest GHG emissions, SSP5-8.5, leads to more significant changes. In both scenarios, a significant increase in wind power density is forecasted over most of mainland Southeast Asia. The scenarios also agree regarding most of Indonesia, with a significant wind power increase being forecast in Java, Sulawesi and the Southern New Guinea.

Nonetheless, some discrepancies are still observed between the projections in different climate change scenarios, with opposite trends in some areas. Whereas the SSP2-4.5 scenario predicts a slight global

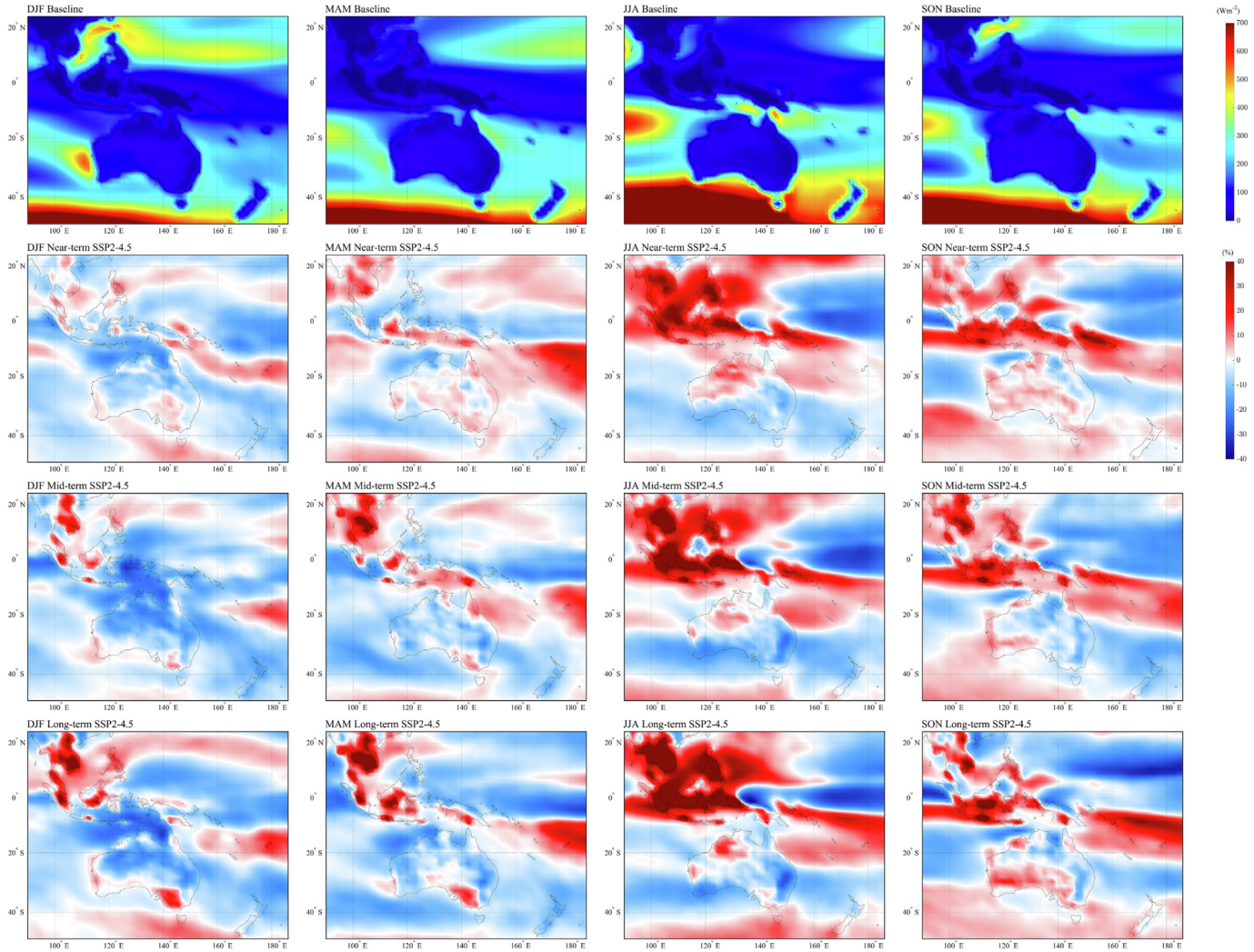

Fig. 6. Baseline values (uppermost row of panels) and evolution of seasonal mean wind power density in the near- (second row of panels), mid- (third row of panels) and long (last row of panels) in the SSP2-4.5 scenario. DJF (December – January – February), MAM (March – April – May), JJA (June – July – August) and SON (September – October – November).

increase in wind power density in the South China Sea and the surrounding landmasses and islands, the SSP5-8.5 anticipates a much more mixed evolution, with a decrease in the Gulf of Thailand, Malaysia and Sumatra and a mixed evolution in the Philippines. New Zealand is another area of discrepancy between the scenarios, with the SSP2-4.5 forecasting a slight decrease overall except for the southwestern tip of South Island, while SSP5-8.5 foresees a significant increase over South Island and a decrease over most of North Island.

Wind projections with the SSPs scenarios show extremely powerful changes in the available wind energy potential focused in specific regions. The remaining regions, conversely, do not show significant deviations from current mean wind conditions. This evolution of the resource is opposite to that evaluated in other large regions with the same SSPs, e.g., Europe (Martinez and Iglesias, 2021b) and North America (Martinez and Iglesias, 2022c), where significant, well-spread changes are anticipated in large areas and no particular region experiencing exceptionally larger changes. This could be a result of large-scale changes in global atmospheric circulation in the Northern Hemisphere against the Southern Hemisphere. Importantly, the concentrated changes highlighted in this work are not reflected in previous works with now-outdated scenarios of climate change (Herrmann et al., 2020; Jung and Schindler, 2019). This could be due to the scenarios themselves, a lack of spatial resolution or the individual uncertainties of using a single-model approach. In any case, the magnitude of the changes in specific regions that are anticipated in this work could change drastically the regional wind energy landscape.

3.2. Coefficient of variation

The general variability of the wind energy potential is evaluated through the coefficient of variation (*COV*) (Walpole et al., 2007):

$$COV = \frac{\sigma}{\mu}, \tag{3}$$

where σ is the standard deviation and μ the mean value of the wind power density over the considered time horizon.

The baseline value and the near-, mid- and long-term evolution of the COV are computed (Fig. 5).

In the baseline, the highest values of the COV can be found in the South China Sea, especially between the Malaysian peninsula and Borneo, in the Philippines and over mainland South-East Asia, except for an area of low variability over parts of Myanmar, Laos and China. Conversely, the

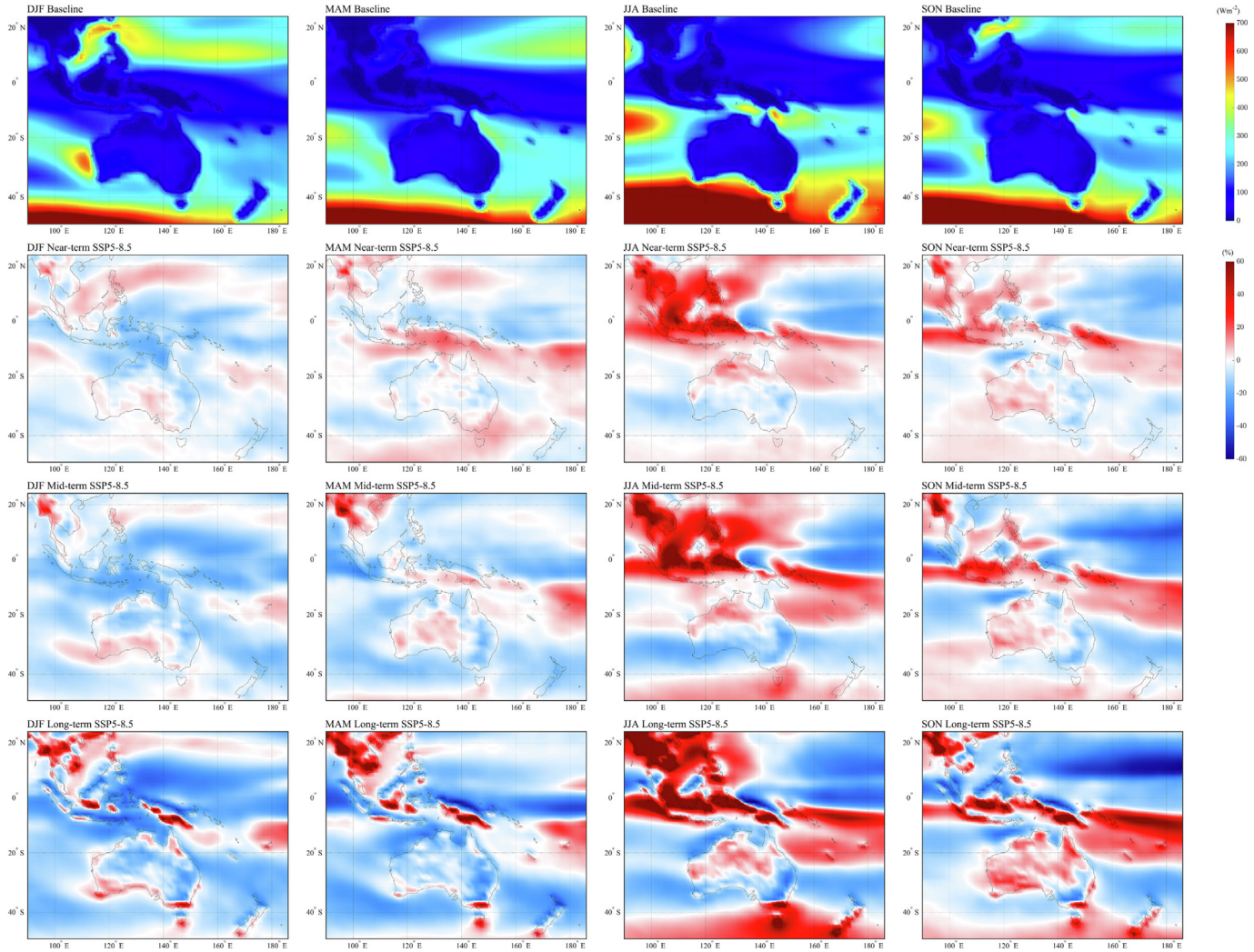

Fig. 7. Baseline values (uppermost row of panels) and evolution of seasonal mean wind power density in the near- (second row of panels), mid- (third row of panels) and long (last row of panels) in the SSP5-8.5 scenario. DJF (December – January – February), MAM (March – April – May), JJA (June – July – August) and SON (September – October – November).

steadiest wind energy potential is found in New Guinea, Borneo, and a small part of the Indian Ocean around 20°S. Australia overall experiences relatively steady winds.

Similarly to the previous section, there is general agreement between the two scenarios (Fig. 5). In both cases, there is a long-term decrease in the COV values of approximately −15 % in the South China Sea, Cambodia and most of Vietnam, whereas Indonesia and Papua New Guinea experience an increase in variability, between 15 % and 25 % depending on the scenario.

No particular trend can be discerned in the evolution of the overall variability in Australasia. Small, intermingled increases and decreases in the values of the COV are anticipated in the overall region. However, a great increase in the values of the COV (15 %) occurs in the long-term future in the overall areas of the Southern Ocean (latitudes below 40°S).

The variability is an important aspect in the optimisation of wind energy harvesting. The predictability of the wind climate is key in the selection of the optimal wind turbine and the estimation of electricity production, which is the revenue of every wind farm project. Therefore, higher values of the COV are often associated with greater costs of capital and, therefore greater values of the levelised cost of energy.

3.3. Seasonal trends

In order to study predicted changes at an intra-annual scale, the mean wind power density is calculated on a seasonal basis, and the results are compared against historical data for both climate change scenarios (Figs. 6 and 7). Similarly to the overall variability, the intra-annual variability influences the selection of the optimal turbine and the ability to predict the potential energy generation, thus of consequence to the levelised cost of energy. The year is divided into four seasons: December – January – February (DJF), March – April – May (MAM), June – July – August (JJA) and September – October – November (SON).

Seasonal effects are particularly visible in the baseline data in the South China Sea, with the wind power density reaching high values, up to 500 Wm^{-2}, in SON and DJF, while remaining below 200 Wm^{-2} in MAM and JJA. The Equator is surrounded by a strip of low wind power density, the intercontinental convergence zone (ITCZ), which is located more to the south (reaching Northern Australia) in DFJ and more to the north (up to the South China Sea) in JJA. Some seasonal variations can be observed over Australia, with higher wind power density in DJF compared to the rest of the year, and minimal values in JJA. It is noteworthy that the Cape York Peninsula and the surrounding waters see the opposite phenomenon, with calmer winds in DJF and maximum wind power density in JJA. Finally, the area affected by the prevailing westerlies becomes larger in JJA, reaching up to 35°S, while it stays below 45°S in DFJ. This affects Tasmania, New Zealand and the Great Australian Bight, which experiences values of wind power density reaching 500 Wm^{-2} in JJA, while they remain below 300 Wm^{-2} the rest of the year.

Changes in intra-annual variability can thus be interpreted as follows. If wind projections anticipate a growth in wind power density occurring in a season with the strongest resource in a particular area, e.g., Australia in JJA, a rise in the intra-annual variability can be expected; and the opposite if decreases are anticipated in the same period. Similarly, if decreases occur in a time period with the weakest resource in an area, e.g., Southeast Asia in JJA, an augmented intra-annual variability is predicted – and the opposite if increases are anticipated in the same period.

In both scenarios, most of Australia experiences an overall increase in wind power density in SON and a decrease in DJF and MAM. The projections in JJA depend on the scenario: in SSP2-4.5 the wind power density over most of Australia tends to decrease, while it increases in SSP5-8.5. Overall, an increased intra-annual variability is predicted.

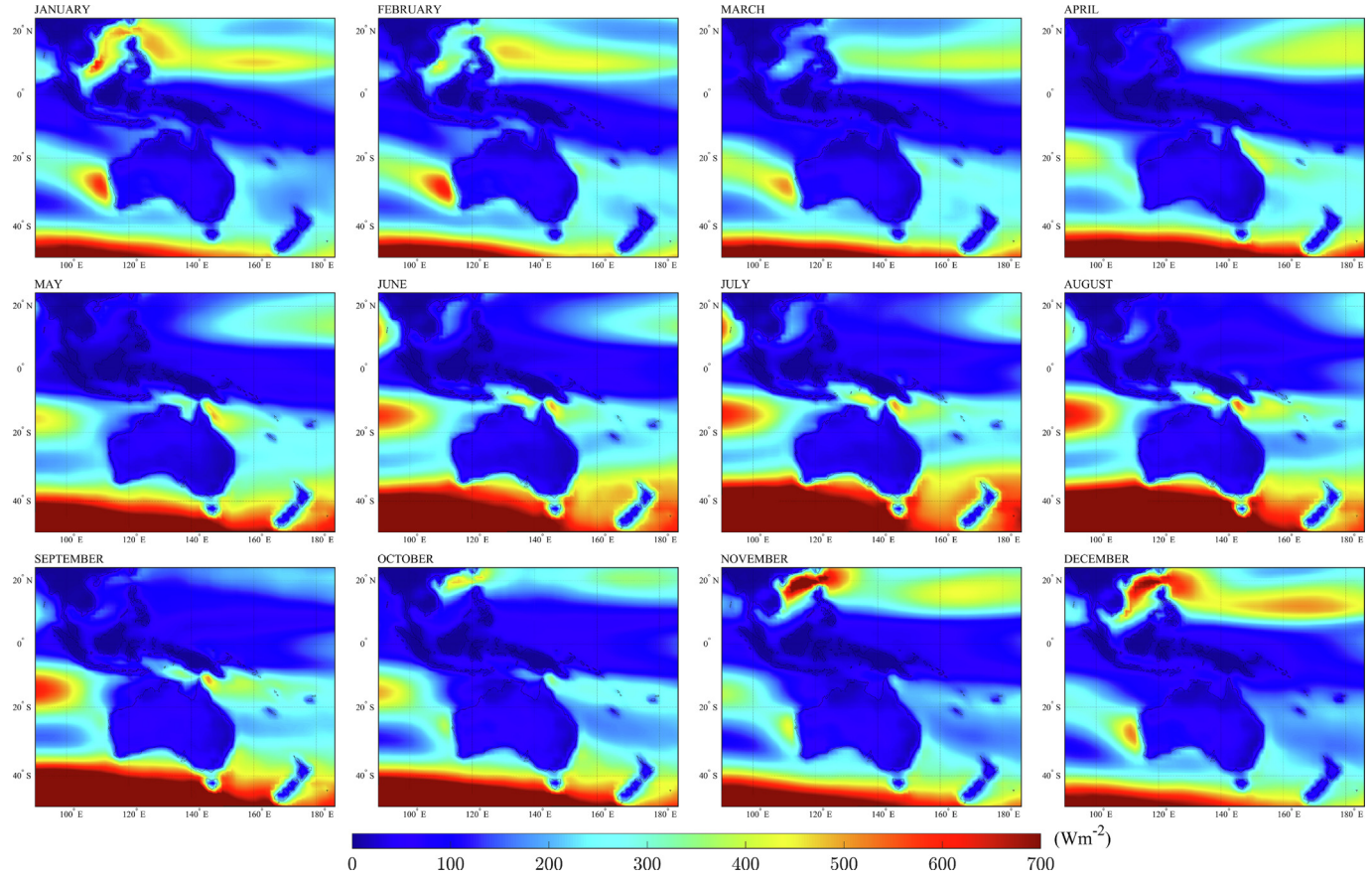

Fig. 8. Baseline values of monthly mean power wind density.

A pronounced seasonal effect can also be observed in South East Asia regardless of the scenario, with a long-term global increase in wind power density over the whole region in JJA, exceeding 100 % in the SSP2-4.5 scenario and 200 % in the SSP5-8.5 scenario in the south of Borneo and in small areas located in Mainland South East Asia – being JJA the period with the weakest resource in the area, a reduced intra-annual variability is anticipated. The rest of the year, however, this area experiences a mix of less pronounced increases and some decreases of up to −40 % locally.

Remarkably, more seasonal variability is projected under the SSP2-4.5 scenario compared to the SSP5-8.5 scenario. For example, in the SSP5-8.5 scenario, the projections anticipate an increase in wind power density that is persistent throughout the year in Myanmar. In Tasmania, the wind power density is projected to increase in the south and decrease in the north. Conversely, the evolution of the wind energy potential is highly season-dependent in these regions in the SSP2-4.5.

3.4. Monthly variability

To evaluate the intra-annual variability of the evolution of the wind energy potential at a finer temporal scale, monthly values of wind power density are calculated in the near, mid and long-term for both climate change scenarios and compared to the baseline data (Figs. 8 to 14).This is possible due to the temporal resolution of the GCMs, a novelty of the CMIP6 – daily-averaged data are employed, enough to conduct a statistically relevant study of monthly trends.

The study of monthly trends is a more refined version of the seasonal scale, and thus results can be interpreted similarly. Increases/decreases in wind power density coinciding with the months with the greatest/weakest, respectively, wind energy potential will lead to an augmented intra-annual variability. Conversely, increases/decreases in wind power density predicted in the months with the weakest/greatest, respectively, wind energy potential will lead to a reduced intra-annual variability.

The near-term changes in wind power density are remarkable for climate change scenarios SSP2-4.5 and SSP5-8.5, with extreme values of −45 % and +60 %, although they do not persist throughout the year. There is general agreement between the projected changes in both scenarios, with similar results on a monthly scale, even though no trend can be discerned.

The monthly variability of the projected changes is especially pronounced in the mid- and long-term in the SSP2-4.5 scenario, e.g., New Zealand sees a slight increase in wind power density from December to May while changes from June to November are more mixed. In most of the region between the Equator and the 5th parallel south, an overall increase in wind power density between May and October is anticipated, while the rest of the year the changes are more mixed - with a slight overall decrease.

Nonetheless, there are some areas with a significant consistency throughout the year: Vietnam presents a year-long increase, with the smallest overall change in October and November, when some regions still see peaks exceeding 50 %, while the highest changes are reached in August - >100 % in some areas. A moderate but persistent decrease in the wind energy potential is anticipated in the Eastern Coast of Australia throughout the year, with the exception of the month of March, where the changes are mixed, with some areas where the wind power density slightly increases.

In the mid- and long-term future in the SSP5-8.5 scenario, the intra-annual variability is less pronounced, while changes in wind power density are more significant. It can be seen that throughout the year, in the southern parts of Borneo, New Guinea and Tasmania an increase throughout the year is anticipated, while a persistent decrease is predicted in the northern parts

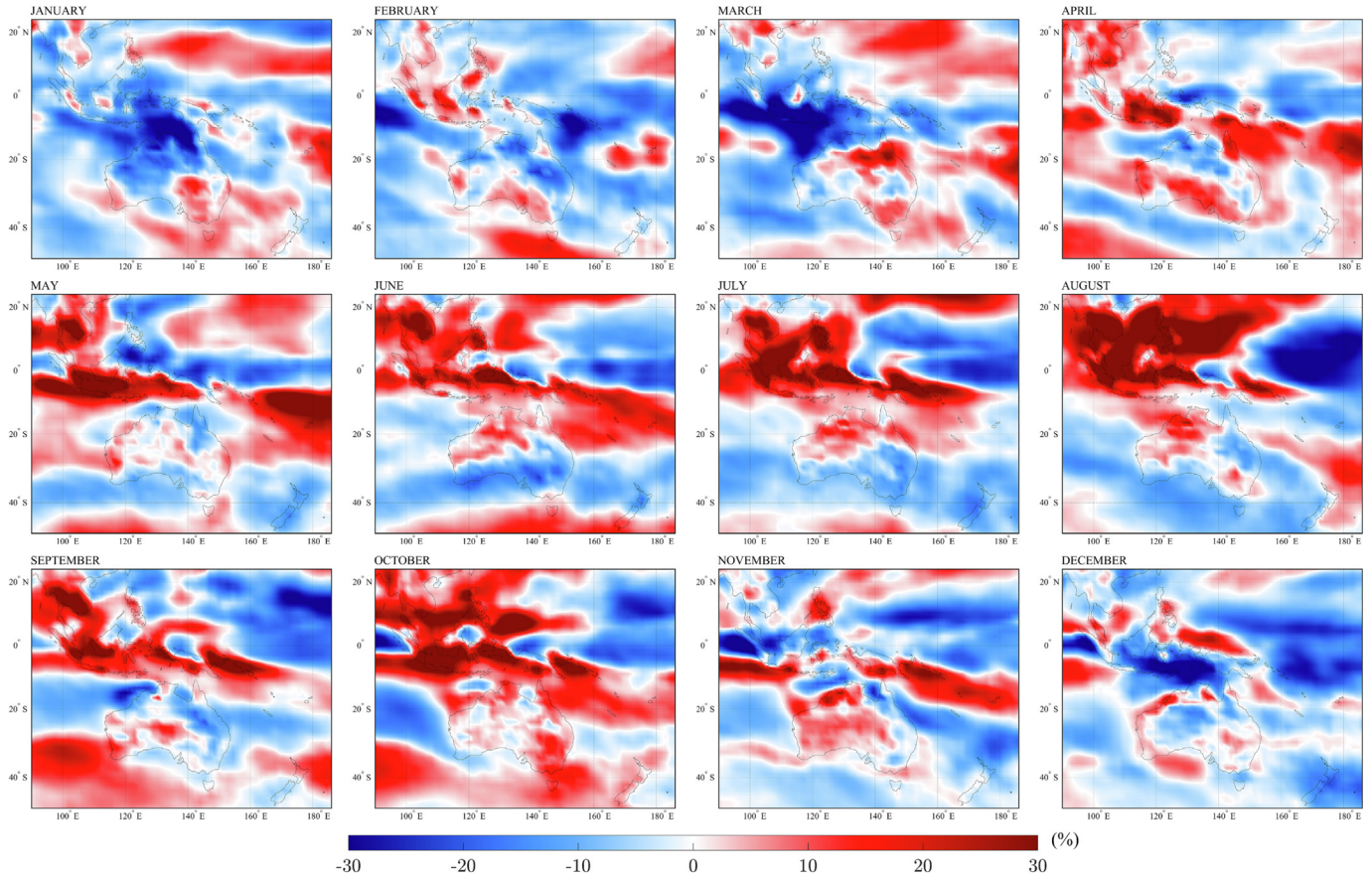

Fig. 9. Near-term evolution of monthly mean power density in the SSP2-4.5 scenario.

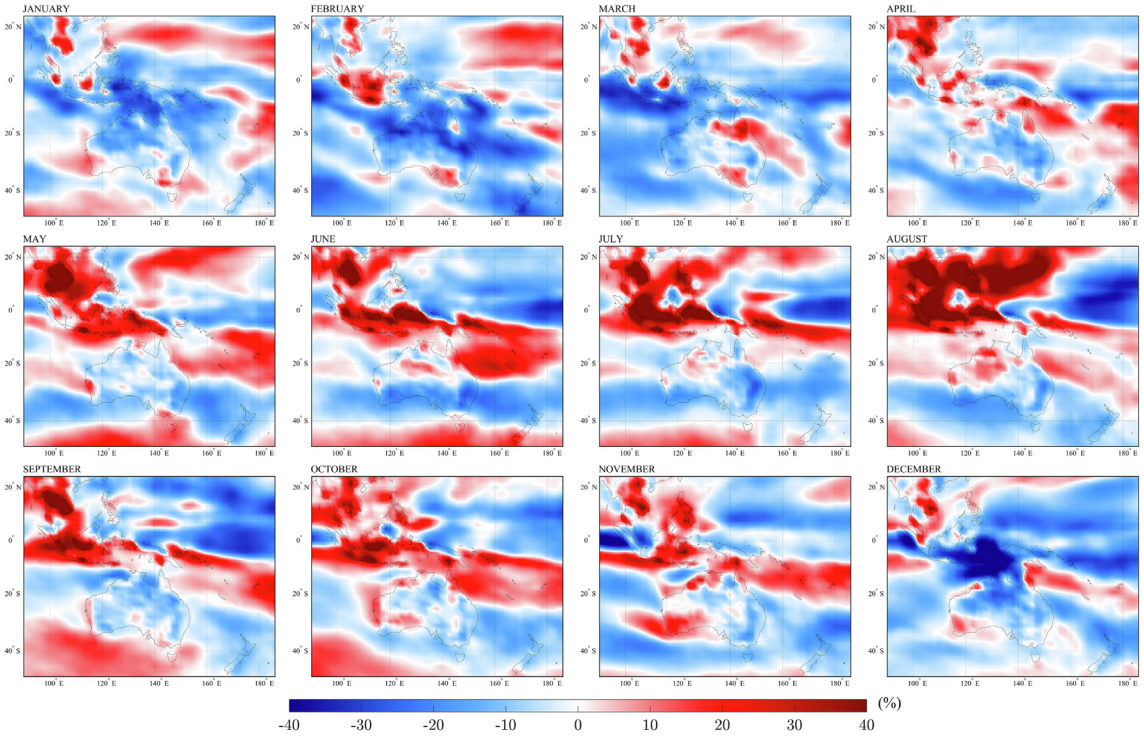

Fig. 10. Mid-term evolution of monthly mean power density in the SSP2-4.5 scenario.

of the two former islands. In New Zealand, the same seasonal variability can be observed as in the SSP2-4.5 scenario, but with a more pronounced intensity. Most regions of Australia also see different changes in wind power density throughout the year, with a global increase between July and November but a global decrease the rest of the year.

4. Conclusion

In this work, the evolution of the wind energy potential is studied for the first time in a region ranging from South-East Asia to Australia and New Zealand based on the most recent climate change scenarios, the

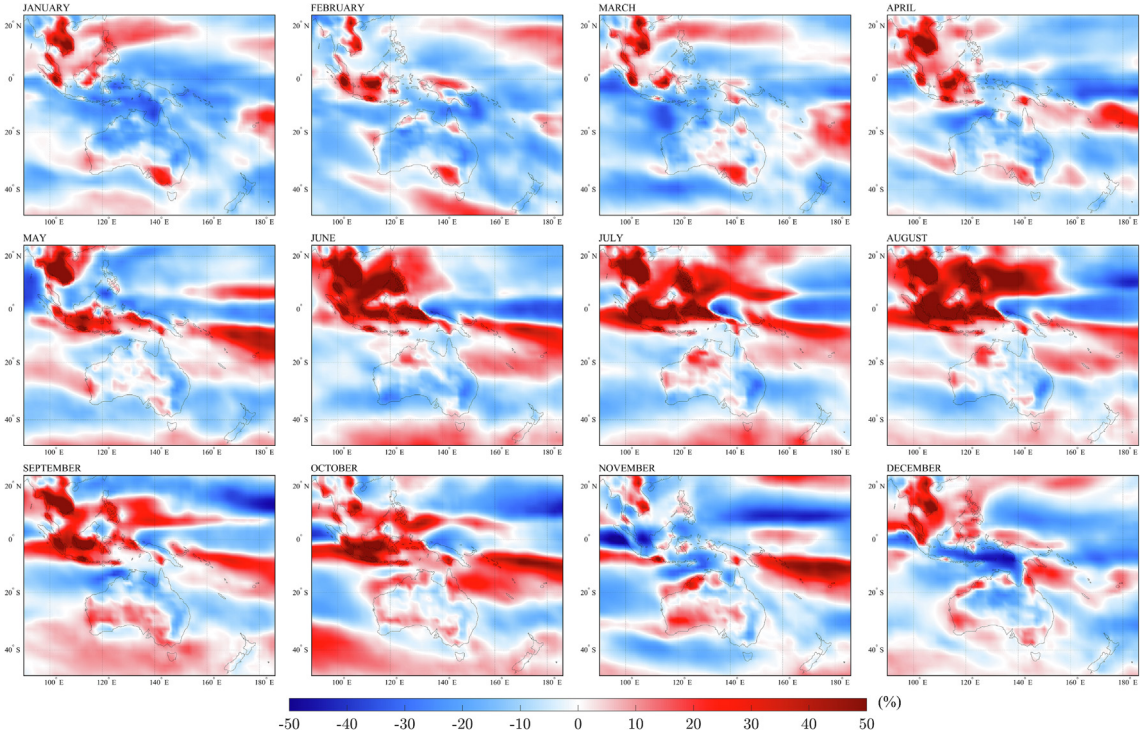

Fig. 11. Long-term evolution of monthly mean power density in the SSP2-4.5 scenario.

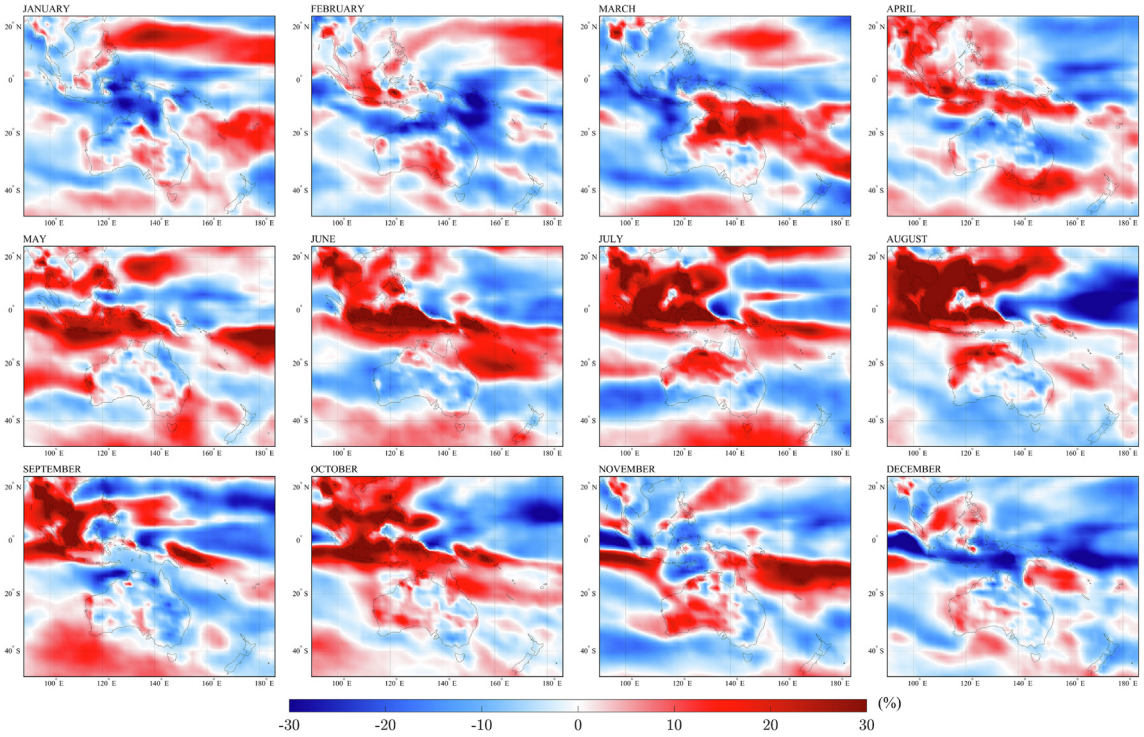

Fig. 12. Near-term evolution of monthly mean power density in the SSP5-8.5 scenario.

SSPs, by constructing a Multi-Model Ensemble with wind climate projections from four different GCMs. The choice of models is based on their performance against past-present data coming from the ERA5 database - a total of 18 GCMs involved in the CMIP6 activities were considered. The data used are based on two Shared Socioeconomic Pathways: the SSP2-4.5, a business-as-usual, intermediate emissions scenario, and the SSP5-8.5, a scenario with high GHG emissions. Three time periods are taken into account: near-term (2022–2031), mid-term (2056–2065) and long-term future (2091–2100).

Although the overall evolution in the area of study is by no means dramatic, significant changes are anticipated in specific regions, e.g., up to +150 % in the southern region of Borneo (up to +200 % in specific

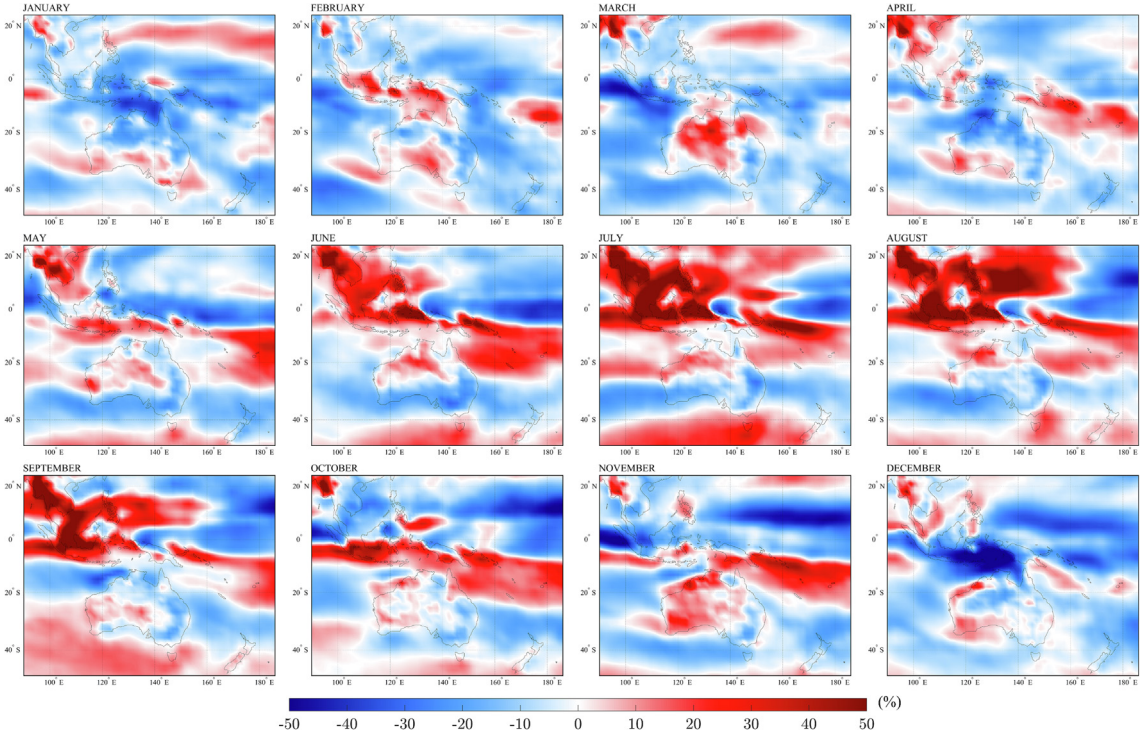

Fig. 13. Mid-term evolution of monthly mean power density in the SSP5-8.5 scenario.

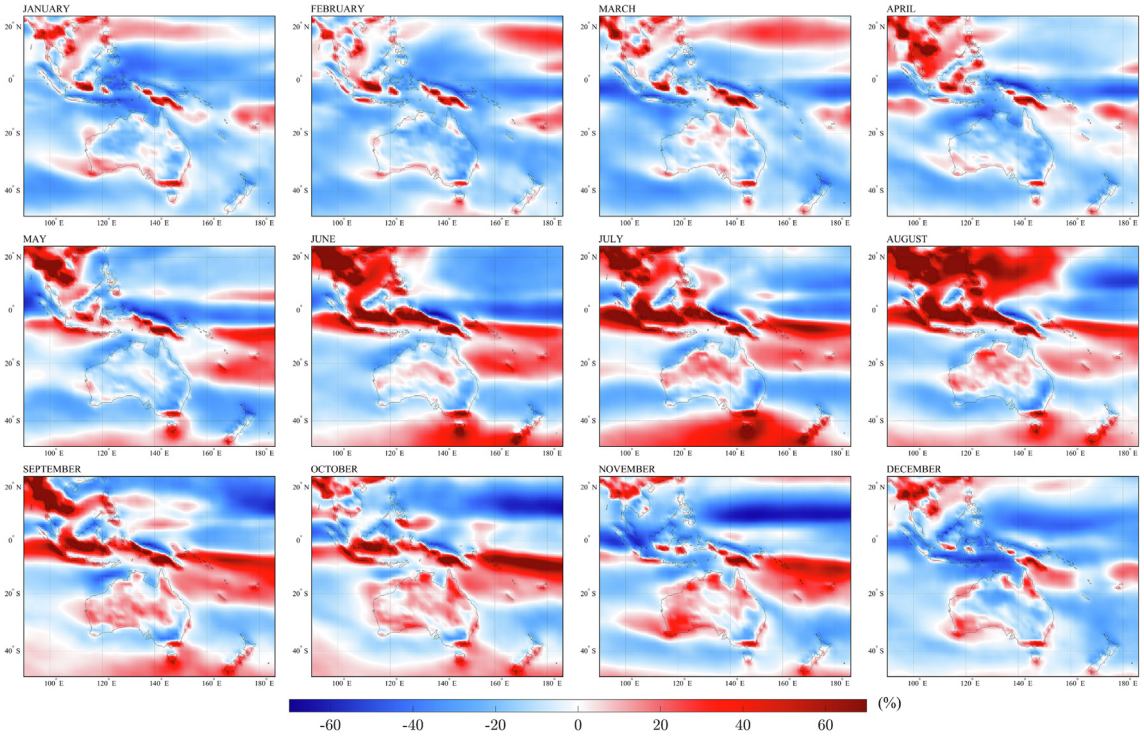

Fig. 14. Long-term evolution of monthly mean power density in the SSP5-8.5 scenario.

months). A significant increase in wind power density is predicted for the South China Sea in the long-term future. These results mark a departure from trends projected for other regions of the world in the literature, in which the anticipated changes are generally distributed more uniformly. In this work, changes of greater magnitude, though localised, have been found in the projections. This may indicate different trends in global atmospheric circulation (Northern Hemisphere against Southern Hemisphere). Moreover, previous works in the same region with now-outdated scenarios of climate change were not able to capture the substantial, concentrated changes in the projected wind energy potential, which may be due to the limitations regarding spatial and temporal resolutions or uncertainties from using a single GCM. As for the overall variability of the resource potential, variations of ±15 % in the COV are well-spread over the region of study.

Both scenarios of climate change show general agreement in the trends in mean wind power and overall variability - for a given region, the evolution is more pronounced in the scenario with the greatest emissions, the SSP5-8.5. However, the study of the intra-annual variability revealed that the SSP2-4.5 predicts greater seasonal variations, in contrast to previous works based on the SSPs in other areas. The intra-annual variability showed remarkable variations in the future wind energy potential. Notable increases were predicted in mainland South East Asia, especially in Vietnam (+100 %) and Borneo (+200 %).

The outcome of this study may be of great relevance for future investments in wind power. This work provided useful insight into large-scale trends of the wind energy potential resulting from climate change. Particularly, this study has identified specific regions in which the wind energy potential is projected to change remarkably, thus affecting the local wind energy industry. The coefficient of variation, particularly, is of great interest to the industry, since it bears great importance in project risk assessment and financing. Projects in places with higher coefficients of variation are harder to finance as investors tend to prefer steadier revenues. Furthermore, specific areas may be selected derived from the findings of this work to be the focus of future downscaling initiatives, especially those areas where substantial, localised variations were identified. Finally, the results presented in this work may motivate future research focusing on economical aspects or extreme events.

CRediT authorship contribution statement

A. Fournier: Conceptualization, Data curation, Formal analysis, Investigation, Methodology, Writing – original draft. **A. Martinez:** Conceptualization, Methodology, Supervision, Validation, Writing – review & editing. **G. Iglesias:** Conceptualization, Methodology, Supervision, Validation, Writing – review & editing.

Data availability

The authors do not have permission to share data.

Declaration of competing interest

The authors declare that they have no known competing financial interests or personal relationships that could have appeared to influence the work reported in this paper.

Acknowledgments

The authors would like to thank the numerous groups and organisations participating in the ScenarioMIP activities of the CMIP6 for producing and making available the data used in this work. The authors are also grateful for the European Center for Medium-Range Weather Forecasts (ECMWF) for making their products available. ERA-5 data on wind speed was downloaded from the Copernicus Climate Change Service (C3S) Climate Data Store. The results contain modified Copernicus Climate Change Service information 2022. Neither the European Commission nor ECMWF is responsible for any use that may be made of the Copernicus information or data it contains. The authors are also grateful to MaREI, the SFI Research Centre for Energy, Climate and Marine research and innovation coordinated by the Environmental Research Institute (ERI) (Grant MAREI2_12/RC/2302/P2 Platform RA1b).

This research was supported by European Union's Horizon 2020 European Green Deal Research and Innovation Program (H2020-LC-GD-2020-4), grant No. 101037643 – ILIAD (Integrated Digital Framework for Comprehensive Maritime Data and Information Services).

References

Arif, M.S., Abodayeh, K., Nawaz, Y., 2022. A computational approach to a mathematical model of climate change using heat sources and diffusion. Civ.Eng.J. 8 (7), 1358–1368.

Astariz, S., Perez-Collazo, C., Abanades, J., Iglesias, G., 2015. Co-located wave-wind farms: economic assessment as a function of layout. Renew. Energy 83, 837–849. https://doi.org/10.1016/j.renene.2015.05.028 https://www.sciencedirect.com/science/article/pii/S0960148115004073.

Bentsen, M., Olivie, D.J.L., Seland, O., Toniazzo, T., Gjermundsen, A., Graff, L.S., Debernard, J.B., Gupta, A.K., He, Y., Kirkevåg, A., Schwinger, J., Tjiputra, J., Aas, K.S., Bethke, I., Fan, Y., Griesfeller, J., Grini, A., Guo, C., Ilicak, M., Karset, I.H.H., Landgren, O.A., Liakka, J., Moseid, K.O., Nummelin, A., Spensberger, C., Tang, H., Zhang, Z., Heinze, C., Iversen, T., Schulz, M., 2019. Ncc noresm2-mm model output prepared for cmip6 cmip historical. https://doi.org/10.22033/ESGF/CMIP6.8040 URL http://cera-www.dkrz.de/WDCC/meta/CMIP6/CMIP6.CMIP.NCC.NorESM2-MM.historical.

Bergillos, R.J., Rodriguez-Delgado, C., Allen, J., Iglesias, G., 2019. Wave energy converter geometry for coastal flooding mitigation. Sci. Total Environ. 668, 1232–1241.

Bloom, A., Kotroni, V., Lagouvardos, K., 2008. Climate change impact of wind energy availability in the eastern Mediterranean using the regional climate model precis. Nat. Hazards Earth Syst. Sci. 8 (6), 1249–1257.

Boucher, O., Denvil, S., Levavasseur, G., Cozic, A., Caubel, A., Foujols, M.-A., Meurdesoif, Y., Cadule, P., Devilliers, M., Dupont, E., Lurton, T., 2019. Ipsl ipsl-cm6a-lr model output prepared for cmip6 scenariomip. https://doi.org/10.22033/ESGF/CMIP6.1532 URL http://cera-www.dkrz.de/WDCC/meta/CMIP6/CMIP6.ScenarioMIP.IPSL.IPSL-CM6A-LR.

Brands, S., Herrera, S., Fernández, J., Gutiérrez, J.M., 2013. How well do CMIP5 earth system models simulate present climate conditions in Europe and Africa? Clim. Dyn. 41 (3–4), 803–817. https://doi.org/10.1007/s00382-013-1742-8.

Byun, Y.-H., Lim, Y.-J., Shim, S., Sung, H.M., Sun, M., Kim, J., Kim, B.-H., Lee, J.-H., Moon, H., 2019. Nims-kma kace1.0-g model output prepared for cmip6 scenariomip. doi:10.22033/ESGF/CMIP6.6693 https://doi.org/10.22033/ESGF/CMIP6.8437.

Carvalho, D., Rocha, A., Gómez-Gesteira, M., Santos, C.S., 2017. Potential impacts of climate change on European wind energy resource under the cmip5 future climate projections. Renew. Energy 101, 29–40.

Cavazzi, S., Dutton, A., 2016. An offshore wind energy geographic information system (OWE-GIS) for assessment of the UK's offshore wind energy potential. Renew. Energy 87, 212–228.

Chancham, C., Waewsak, J., Gagnon, Y., 2017. Offshore wind resource assessment and wind power plant optimization in the Gulf of Thailand. Energy 139, 706–731. https://doi.org/10.1016/j.energy.2017.08.026 https://www.sciencedirect.com/science/article/pii/S0360544217314019.

Château, P.-A., Chang, Y.-C., Chen, H., Ko, T.-T., 2012. Building a stakeholder's vision of an offshore wind-farm project: a group modeling approach. Sci. Total Environ. 420, 43–53.

Danabasoglu, G., 2019. Ncar cesm2-waccm model output prepared for cmip6 scenariomip. https://doi.org/10.22033/ESGF/CMIP6.10026 URL http://cera-www.dkrz.de/WDCC/meta/CMIP6/CMIP6.ScenarioMIP.NCAR.CESM2-WACCM.

Dinh, V.N., Leahy, P., McKeogh, E., Murphy, J., Cummins, V., 2021. Development of a viability assessment model for hydrogen production from dedicated offshore wind farms. doi:10.22033/ESGF/CMIP6.6693Int. J. Hydrog. Energy 46 (48), 24620–24631.

Dix, M., Bi, D., Dobrohotoff, P., Fiedler, R., Harman, I., Law, R., Mackallah, C., Marsland, S., O'Farrell, S., Rashid, H., Srbinovsky, J., Sullivan, A., Trenham, C., Vohralik, P., Watterson, I., Williams, G., Woodhouse, M., Bodman, R., Dias, F.B., Domingues, C., Hannah, N., Heerdegen, A., Savita, A., Wales, S., Allen, C., Druken, K., Evans, B., Richards, C., Ridzwan, S.M., Roberts, D., Smillie, J., Snow, K., Ward, M., Yang, R., 2019. Csiro-arccss access-cm2 model output prepared for cmip6 scenariomip ssp245. https://doi.org/10.22033/ESGF/CMIP6.4321 URL http://cera-www.dkrz.de/WDCC/meta/CMIP6/CMIP6.ScenarioMIP.AWI.AWI-CM-1-1-MR.

Dix, M., Bi, D., Dobrohotoff, P., Fiedler, R., Harman, I., Law, R., Mackallah, C., Marsland, S., O'Farrell, S., Rashid, H., Srbinovsky, J., Sullivan, A., Trenham, C., Vohralik, P., Watterson, I., Williams, G., Woodhouse, M., Bodman, R., Dias, F.B., Domingues, C., Hannah, N., Heerdegen, A., Savita, A., Wales, S., Allen, C., Druken, K., Evans, B., Richards, C., Ridzwan, S.M., Roberts, D., Smillie, J., Snow, K., Ward, M., Yang, R., 2019. Csiro-arccss access-cm2 model output prepared for cmip6 scenariomip ssp585. doi:10.22033/ESGF/CMIP6.6705 https://doi.org/10.22033/ESGF/CMIP6.4332.

Dosio, A., Panitz, H.-J., Schubert-Frisius, M., Lüthi, D., 2015. Dynamical downscaling of cmip5 global circulation models over cordex-Africa with cosmo-clm: evaluation over the present climate and analysis of the added value. Clim. Dyn. 44, 2637–2661.

EC-Earth Consortium (EC-Earth), 2019. Ec-earth-consortium ec-earth3 model output prepared for cmip6 scenariomip ssp245. https://doi.org/10.22033/ESGF/CMIP6.4880 URL http://cera-www.dkrz.de/WDCC/meta/CMIP6/CMIP6.ScenarioMIP.EC-Earth-Consortium.EC-Earth3.ssp245.

Erdiwansyah, Mamat, R., Sani, M., Sudhakar, K., 2019. Renewable energy in Southeast Asia: policies and recommendations. Sci. Total Environ. 670, 1095–1102. https://doi.org/10.1016/j.scitotenv.2019.03.273 URL https://www.sciencedirect.com/science/article/pii/S0048969719312653.

Eyring, V., Bony, S., Meehl, G.A., Senior, C.A., Stevens, B., Stouffer, R.J., Taylor, K.E., 2016. Overview of the coupled model intercomparison project phase 6 (CMIP6) experimental design and organization. 9 (5), pp. 1937–1958. https://doi.org/10.5194/gmd-9-1937-2016 URL doi:10.5194/gmd-9-1937-2016.

Foley, A.M., Leahy, P., McKeogh, E., 2010. Wind power forecasting prediction methods. 2010 9th International Conference on Environment And Electrical Engineering, pp. 61–64 https://doi.org/10.1109/EEEIC.2010.5490016.

Foley, A.M., Leahy, P.G., Marvuglia, A., McKeogh, E.J., 2012. Current methods and advances in forecasting of wind power generation. Renew. Energy 37 (1), 1–8. https://doi.org/10.1016/j.renene.2011.05.033 https://www.sciencedirect.com/science/article/pii/S0960148111002850.

Fyrippis, I., Axaopoulos, P.J., Panayiotou, G., 2010. Wind energy potential assessment in Naxos Island, Greece. Appl. Energy 87 (2), 577–586.

G. Global Wind Energy Council, 2021. Global Wind Report 2021.

G. Global Wind Energy Council, 2022. Global Wind Report 2022 URL http://cera-www.dkrz.de/WDCC/meta/CMIP6/CMIP6.ScenarioMIP.MRI.MRI-ESM2-0.

Gualtieri, G., 2021. Reliability of era5 reanalysis data for wind resource assessment: a comparison against tall towers. Energies 14 (14), 4169.

Guo, H., John, J.G., Blanton, C., McHugh, C., Nikonov, S., Radhakrishnan, A., Rand, K., Zadeh, N.T., Balaji, V., Durachta, J., Dupuis, C., Menzel, R., Robinson, T., Underwood, S., Vahlenkamp, H., Dunne, K.A., Gauthier, P.P., Ginoux, P., Griffies, S.M., Hallberg, R., Harrison, M., Hurlin, W., Lin, P., Malyshev, S., Naik, V., Paulot, F., Paynter, D.J., Ploshay, J., Schwarzkopf, D.M., Seman, C.J., Shao, A., Silvers, L., Wyman, B., Yan, X., Zeng, Y., Adcroft, A., Dunne, J.P., Held, I.M., Krasting, J.P., Horowitz, L.W., Milly, C., Shevliakova, E., Winton, M., Zhao, M., Zhang, R., 2018. Noaa-gfdl gfdl-cm4 model output prepared for cmip6 scenariomip. doi:10.22033/ESGF/CMIP6.9242 http://cera-www.dkrz.de/WDCC/meta/CMIP6/CMIP6.ScenarioMIP.NOAA-GFDL.GFDL-CM4.

Guthrie, W.F., 2020. Nist/sematech e-handbook of statistical methods (nist handbook 151). doi:10.22033/ESGF/CMIP6.6705 https://doi.org/10.18434/M32189.

Gutowski Jr., W.J., Giorgi Jr., F., Timbal Jr., B., Frigon Jr., A., Jacob Jr., D., Kang Jr., H.-S., Krishnan Jr., R., Lee Jr., B., Lennard Jr., C., Nikulin Jr., G., et al., 2016. Wcrp coordinated regional downscaling experiment (cordex): a diagnostic mip for cmip6.

Herrmann, M., Ngo-Duc, T., Trinh-Tuan, L., 2020. Impact of climate change on sea surface wind in Southeast Asia, from climatological average to extreme events: results from a dynamical downscaling. Clim. Dyn. 54 (3–4), 2101–2134. https://doi.org/10.1007/s00382-019-05103-6 URL doi:10.1007/s00382-019-05103-6.

Hersbach, H., Dee, D., 2016. Era5 reanalysis is in production. ECMWF Newsl. 147 (7), 5–6.

IPCC, 2021. Climate Change 2021: The Physical Science Basis. Contribution of Working Group I to the Sixth Assessment Report of the Intergovernmental Panel on Climate Change. Cambridge University Press.

John, J.G., Blanton, C., McHugh, C., Radhakrishnan, A., Rand, K., Vahlenkamp, H., Wilson, C., Zadeh, N.T., Dunne, J.P., Dussin, R., Horowitz, L.W., Krasting, J.P., Lin, P., Malyshev, S., Naik, V., Ploshay, J., Shevliakova, E., Silvers, L., Stock, C., Winton, M., Zeng, Y., 2018. Noaa-gfdl gfdl-esm4 model output prepared for cmip6 scenariomip. https://doi.org/10.22033/ESGF/CMIP6.1414 URL http://cera-www.dkrz.de/WDCC/meta/CMIP6/CMIP6.ScenarioMIP.NOAA-GFDL.GFDL-ESM4.

Jones, P.W., 1999. First- and second-order conservative remapping schemes for grids in spherical coordinates. Mon. Weather Rev. 127 (9), 2204–2210. https://doi.org/10.1175/1520-0493(1999)127<2204:fasocr>2.0.co;2 URL doi:10.1175/1520-0493(1999)127<2204:fasocr>2.0.co;2.

Jonkman, J., Matha, D., 2010. Quantitative Comparison of the Responses of Three Floating Platforms, Tech. rep. National Renewable Energy Lab.(NREL), Golden, CO (United States).

Jung, C., Schindler, D., 2019. Changing wind speed distributions under future global climate. Energy Convers. Manag. 198, 111841. https://doi.org/10.1016/j.enconman.2019.111841 URL doi:10.1016/j.enconman.2019.111841.

Lavidas, G., Venugopal, V., 2018. Energy production benefits by wind and wave energies for the autonomous system of Crete. Energies 11 (10). https://doi.org/10.3390/en11102741 https://www.mdpi.com/1996-1073/11/10/2741 https://www.mdpi.com/1996-1073/11/10/2741.

Lee, J., Zhao, F., Dutton, A., Backwell, B., Fiestas, R., Qiao, L., Balachandran, N., Lim, S., Liang, W., Clarke, E., Lathigara, A., Younger, D.R., 2021. Global Wind Report 2021, Tech. rep. Global Wind Energy Council.

Liao, H., Chang, W., 2014. Integrated assessment of air quality and climate change for policy-making: highlights of ipcc ar5 and research challenges. Natl. Sci. Rev. 1 (2), 176–179.

López, M., Rodríguez-Fuertes, N., Carballo, R., 2018. Offshore wind energy resource atlas of Asturias (n Spain). Proceedings 2 (23). https://doi.org/10.3390/proceedings2231416 URL https://www.mdpi.com/2504-3900/2/23/1416.

López, M., Rodríguez, N., Iglesias, G., 2020. Combined floating offshore wind and solar pv. J. Mar.Sci.Eng. 8 (8). https://doi.org/10.3390/jmse8080576 https://www.mdpi.com/2077-1312/8/8/576 https://www.mdpi.com/2077-1312/8/8/576.

Martinez, A., Iglesias, G., 2020. Wave exploitability index and wave resource classification. Renew. Sust. Energ. Rev. 134, 110393.

Martinez, A., Iglesias, G., 2021. Multi-parameter analysis and mapping of the levelised cost of energy from floating offshore wind in the Mediterranean sea. Energy Convers. Manag. 243, 114416. https://doi.org/10.1016/j.enconman.2021.114416 https://www.sciencedirect.com/science/article/pii/S0196890421005926.

Martinez, A., Iglesias, G., 2021. Wind resource evolution in Europe under different scenarios of climate change characterised by the novel shared socioeconomic pathways. Energy Convers. Manag. 234, 113961. https://doi.org/10.1016/j.enconman.2021.113961 URL doi:10.1016/j.enconman.2021.113961.

Martinez, A., Iglesias, G., 2022. Mapping of the levelised cost of energy for floating offshore wind in the European Atlantic. Renew. Sust. Energ. Rev. 154, 111889. https://doi.org/10.1016/j.rser.2021.111889 https://www.sciencedirect.com/science/article/pii/S1364032121011564.

Martinez, A., Iglesias, G., 2022. Site selection of floating offshore wind through the levelised cost of energy: a case study in Ireland. Energy Convers. Manag. 266, 115802. https://doi.org/10.1016/j.enconman.2022.115802 https://www.sciencedirect.com/science/article/pii/S0196890422005982.

Martinez, A., Iglesias, G., 2022. Climate change impacts on wind energy resources in North America based on the CMIP6 projections. Sci. Total Environ. 806, 150580. https://doi.org/10.1016/j.scitotenv.2021.150580 URL doi:10.1016/j.scitotenv.2021.150580.

Martinez, A., Murphy, L., Iglesias, G., 2023. Evolution of offshore wind resources in northern Europe under climate change. Energy, 126655 https://doi.org/10.1016/j.energy.2023.126655 https://www.sciencedirect.com/science/article/pii/S036054422300049X https://www.sciencedirect.com/science/article/pii/S036054422300049X.

Moradian, S., Akbari, M., Iglesias, G., 2022. Optimized hybrid ensemble technique for cmip6 wind data projections under different climate-change scenarios. Case study: United Kingdom. Sci. Total Environ. 826, 154124. https://doi.org/10.1016/j.scitotenv.2022.154124 https://www.sciencedirect.com/science/article/pii/S0048969722012165 https://www.sciencedirect.com/science/article/pii/S0048969722012165.

Moradian, S., Haghighi, A.Torabi, Asadi, M., Mirbagheri, S.A., 2022. Future changes in precipitation over northern Europe based on a multi-model ensemble from cmip6: Focus on tana river basin. doi:10.22033/ESGF/CMIP6.9242Water Resour. Manag. 1–17.

Pavlova, A., Myslenkov, S., Arkhipkin, V., Surkova, G., 2022. Storm surges and extreme wind waves in the Caspian Sea in the present and future climate. Civ.Eng.J. 8 (11), 2353–2377.

Perez-Collazo, C., Greaves, D., Iglesias, G., 2018. A novel hybrid wind-wave energy converter for jacket-frame substructures. Energies 11 (3). https://doi.org/10.3390/en11030637 https://www.mdpi.com/1996-1073/11/3/637 https://www.mdpi.com/1996-1073/11/3/637.

Perez-Collazo, C., Pemberton, R., Greaves, D., Iglesias, G., 2019. Monopile-mounted wave energy converter for a hybrid wind-wave system. Energy Convers. Manag. 199, 111971. https://doi.org/10.1016/j.enconman.2019.111971 https://www.sciencedirect.com/science/article/pii/S019689041930977X.

Pierce, D.W., Barnett, T.P., Santer, B.D., Gleckler, P.J., 2009. Selecting global climate models for regional climate change studies. Proc. Natl. Acad. Sci. 106 (21), 8441–8446 arXiv: https://www.pnas.org/content/106/21/8441.full.pdf, doi:10.1073/pnas.0900094106. URL https://www.pnas.org/content/106/21/8441.

Pınarbaşı, K., Galparsoro, I., Depellegrin, D., Bald, J., Pérez-Morán, G., Borja, Á., 2019. A modelling approach for offshore wind farm feasibility with respect to ecosystem-based marine spatial planning. Sci. Total Environ. 667, 306–317.

Qian, H., Zhang, R., 2020. Future changes in wind energy resource over the northwest passage based on the cmip6 climate projections. Int. J. Energy Res. 45 (1), 920–937. https://doi.org/10.1002/er.5997 URL doi:10.1002/er.5997.

Ramos, V., Giannini, G., Calheiros-Cabral, T., López, M., Rosa-Santos, P., Taveira-Pinto, F., 2022. Assessing the effectiveness of a novel WEC concept as a co-located solution for offshore wind farms. J.Mar.Sci.Eng. 10 (2). https://doi.org/10.3390/jmse10020267 https://www.mdpi.com/2077-1312/10/2/267 https://www.mdpi.com/2077-1312/10/2/267.

Renewables 2020, Tech. rep. International Energy Agency.

Riahi, K., van Vuuren, D.P., Kriegler, E., Edmonds, J., O'Neill, B.C., Fujimori, S., Bauer, N., Calvin, K., Dellink, R., Fricko, O., Lutz, W., Popp, A., Cuaresma, J.C., KC, S., Leimbach, M., Jiang, L., Kram, T., Rao, S., Emmerling, J., Ebi, K., Hasegawa, T., Havlik, P., Humpenöder, F., Silva, L.A.D., Smith, S., Stehfest, E., Bosetti, V., Eom, J., Gernaat, D., Masui, T., Rogelj, J., Strefler, J., Drouet, L., Krey, V., Luderer, G., Harmsen, M., Takahashi, K., Baumstark, L., Doelman, J.C., Kainuma, M., Klimont, Z., Marangoni, G., Lotze-Campen, H., Obersteiner, M., Tabeau, A., Tavoni, M., 2017. The shared socioeconomic pathways and their energy, land use, and greenhouse gas emissions implications: an overview. 42, pp. 153–168. https://doi.org/10.1016/j.gloenvcha.2016.05.009 URL doi:10.1016/j.gloenvcha.2016.05.009.

Rodriguez-Delgado, C., Bergillos, R.J., Ortega-Sánchez, M., Iglesias, G., 2018. Wave farm effects on the coast: the alongshore position. Sci. Total Environ. 640, 1176–1186.

Schupfner, M., Wieners, K.-H., Wachsmann, F., Steger, C., Bittner, M., Jungclaus, J., Früh, B., Pankatz, K., Giorgetta, M., Reick, C., Legutke, S., Esch, M., Gayler, V., Haak, H., de Vrese, P., Raddatz, T., Mauritsen, T., von Storch, J.-S., Behrens, J., Brovkin, V., Claussen, M., Crueger, T., Fast, I., Fiedler, S., Hagemann, S., Hohenegger, C., Jahns, T., Kloster, S., Kinne, S., Lasslop, G., Kornblueh, L., Marotzke, J., Matei, D., Meraner, K., Mikolajewicz, U., Modali, K., Müller, W., Nabel, J., Notz, D., Peters, K., Pincus, R., Pohlmann, H., Pongratz, J., Rast, S., Schmidt, H., Schnur, R., Schulzweida, U., Six, K., Stevens, B., Voigt, A., Roeckner, E., 2019. Dkrz mpi-esm1.2-hr model output prepared for cmip6 scenariomip ssp585. https://doi.org/10.22033/ESGF/CMIP6.4403 URL https://www.sciencedirect.com/science/article/pii/S0048969719312653.

Semmler, T., Danilov, S., Rackow, T., Sidorenko, D., Barbi, D., Hegewald, J., Pradhan, H.K., Sein, D., Wang, Q., Jung, T., 2019. Awi awi-cm1.1mr model output prepared for cmip6 scenariomip. https://doi.org/10.22033/ESGF/CMIP6.376 URL http://cera-www.dkrz.de/WDCC/meta/CMIP6/CMIP6.ScenarioMIP.AWI.AWI-CM-1-1-MR.

Shiogama, H., Abe, M., Tatebe, H., 2019. Miroc miroc6 model output prepared for cmip6 scenariomip. https://doi.org/10.22033/ESGF/CMIP6.898 URL http://cera-www.dkrz.de/WDCC/meta/CMIP6/CMIP6.ScenarioMIP.MIROC.MIROC6.

Staschus, K., Kielichowska, I., Ramaekers, L., Wouters, C., Vree, B., Lejarreta, A.V., Sijtsma, L., Krönert, G.N.B.F., Lindroth, S., Yeomans, G.R., 2020. SWECO, Study on the offshore grid potential in the mediterranean region.

Stelzenmüller, V., Gimpel, A., Haslob, H., Letschert, J., Berkenhagen, J., Brüning, S., 2021. Sustainable co-location solutions for offshore wind farms and fisheries need to account for socio-ecological trade-offs. Sci. Total Environ. 776, 145918.

Swart, N.C., Cole, J.N., Kharin, V.V., Lazare, M., Scinocca, J.F., Gillett, N.P., Anstey, J., Arora, V., Christian, J.R., Jiao, Y., Lee, W.G., Majaess, F., Saenko, O.A., Seiler, C., Seinen, C., Shao, A., Solheim, L., von Salzen, K., Yang, D., Winter, B., Sigmond, M., 2019. Cccma canesm5 model output prepared for cmip6 scenariomip. https://doi.org/10.22033/ESGF/CMIP6.1317 URL http://cera-www.dkrz.de/WDCC/meta/CMIP6/CMIP6.ScenarioMIP.CCCma.CanESM5.

Taylor, K.E., Stouffer, R.J., Meehl, G.A., 2012. An overview of CMIP5 and the experiment design. Bull. Am. Meteorol. Soc. 93 (4), 485–498. https://doi.org/10.1175/bams-d-11-00094.1 URL doi:10.1175/bams-d-11-00094.1.

Tebaldi, C., Knutti, R., 2007. The use of the multi-model ensemble in probabilistic climate projections. Phil. Trans. R. Soc. A 365 (1857), 2053–2075. https://doi.org/10.1098/rsta.2007.2076.

Ulazia, A., Saenz, J., Ibarra-Berastegui, G., 2016. Sensitivity to the use of 3dvar data assimilation in a mesoscale model for estimating offshore wind energy potential. A case study of the Iberian northern coastline. Appl. Energy 180, 617–627. https://doi.org/10.1016/j.apenergy.2016.08.033 https://www.sciencedirect.com/science/article/pii/S0306261916311205 https://www.sciencedirect.com/science/article/pii/S0306261916311205.

Ulazia, A., Sáenz, J., Ibarra-Berastegui, G., González-Rojí, S.J., Carreno-Madinabeitia, S., 2017. Using 3dvar data assimilation to measure offshore wind energy potential at different turbine heights in the west Mediterranean. Appl. Energy 208, 1232–1245. https://doi.org/10.1016/j.apenergy.2017.09.030 https://www.sciencedirect.com/science/article/pii/S0306261917313144.

Ulazia, A., Sáenz, J., Ibarra-Berastegi, G., González-Rojí, S.J., Carreno-Madinabeitia, S., 2019. Global estimations of wind energy potential considering seasonal air density changes. Energy 187, 115938. https://doi.org/10.1016/j.energy.2019.115938 https://www.sciencedirect.com/science/article/pii/S0360544219316226.

United Nations, .. List of parties that signed the Paris Agreement on 22 April https://www.un.org/sustainabledevelopment/blog/2016/04/parisagreementsingatures/ accessed: 2022-05-11.

Van Vuuren, D.P., O'Neill, B.C., 2006. The consistency of ipcc's sres scenarios to 1990–2000 trends and recent projections. Clim. Chang. 75 (1–2), 9–46.

Veigas, M., Iglesias, G., 2013. Wave and offshore wind potential for the island of Tenerife. Energy Convers. Manag. 76, 738–745. https://doi.org/10.1016/j.enconman.2013.08.020 https://www.sciencedirect.com/science/article/pii/S0196890413004792.

Veigas, M., Iglesias, G., 2014. Potentials of a hybrid offshore farm for the island of Fuerteventura. Energy Convers. Manag. 86, 300–308. https://doi.org/10.1016/j.enconman.2014.05.032 https://www.sciencedirect.com/science/article/pii/S0196890414004439.

Veigas, M., Ramos, V., Iglesias, G., 2014. A wave farm for an island: detailed effects on the nearshore wave climate. Energy 69, 801–812.

Volodin, E., Mortikov, E., Gritsun, A., Lykossov, V., Galin, V., Diansky, N., Gusev, A., Kostrykin, S., Iakovlev, N., Shestakova, A., Emelina, S., 2019. Inm inm-cm4-8 model output prepared for cmip6 scenariomip ssp245. https://doi.org/10.22033/ESGF/CMIP6.12327 URL https://doi.org/10.22033/ESGF/CMIP6.12327.

Volodin, E., Mortikov, E., Gritsun, A., Lykossov, V., Galin, V., Diansky, N., Gusev, A., Kostrykin, S., Iakovlev, N., Shestakova, A., Emelina, S., 2019. Inm inm-cm4-8 model output prepared for cmip6 scenariomip ssp585. https://doi.org/10.22033/ESGF/CMIP6.12337 URL https://doi.org/10.22033/ESGF/CMIP6.12337.

Volodin, E., Mortikov, E., Gritsun, A., Lykossov, V., Galin, V., Diansky, N., Gusev, A., Kostrykin, S., Iakovlev, N., Shestakova, A., Emelina, S., 2019. Inm inm-cm5-0 model output prepared for cmip6 scenariomip ssp245. https://doi.org/10.22033/ESGF/CMIP6.12328 URL http://cera-www.dkrz.de/WDCC/meta/CMIP6/CMIP6.ScenarioMIP.INM.INM-CM5-0.ssp245.

Volodin, E., Mortikov, E., Gritsun, A., Lykossov, V., Galin, V., Diansky, N., Gusev, A., Kostrykin, S., Iakovlev, N., Shestakova, A., Emelina, S., 2019. Inm inm-cm5-0 model output prepared for cmip6 scenariomip ssp585. https://doi.org/10.22033/ESGF/CMIP6.12338 URL http://cera-www.dkrz.de/WDCC/meta/CMIP6/CMIP6.ScenarioMIP.INM.INM-CM5-0.ssp585.

Walpole, R.E., Myers, R.H., Myers, S.L., Ye, K., 2007. Probability & Statistics for Engineers And Scientists. 8th edition. Pearson Education, Upper Saddle River.

Wieners, K.-H., Giorgetta, M., Jungclaus, J., Reick, C., Esch, M., Bittner, M., Gayler, V., Haak, H., de Vrese, P., Raddatz, T., Mauritsen, T., von Storch, J.-S., Behrens, J., Brovkin, V., Claussen, M., Crueger, T., Fast, I., Fiedler, S., Hagemann, S., Hohenegger, C., Jahns, T., Kloster, S., Kinne, S., Lasslop, G., Kornblueh, L., Marotzke, J., Matei, D., Meraner, K., Mikolajewicz, U., Modali, K., Müller, W., Nabel, J., Notz, D., Peters, K., Pincus, R., Pohlmann, H., Pongratz, J., Rast, S., Schmidt, H., Schnur, R., Schulzweida, U., Six, K., Stevens, B., Voigt, A., Roeckner, E., 2019. Mpi-m mpi-esm1.2-lr model output prepared for cmip6 scenariomip ssp245. doi:10.22033/ESGF/CMIP6.6693 http://cera-www.dkrz.de/WDCC/meta/CMIP6/CMIP6.ScenarioMIP.MPI-M.MPI-ESM1-2-LR.ssp245.

Wieners, K.-H., Giorgetta, M., Jungclaus, J., Reick, C., Esch, M., Bittner, M., Gayler, V., Haak, H., de Vrese, P., Raddatz, T., Mauritsen, T., von Storch, J.-S., Behrens, J., Brovkin, V., Claussen, M., Crueger, T., Fast, I., Fiedler, S., Hagemann, S., Hohenegger, C., Jahns, T., Kloster, S., Kinne, S., Lasslop, G., Kornblueh, L., Marotzke, J., Matei, D., Meraner, K., Mikolajewicz, U., Modali, K., Müller, W., Nabel, J., Notz, D., Peters, K., Pincus, R., Pohlmann, H., Pongratz, J., Rast, S., Schmidt, H., Schnur, R., Schulzweida, U., Six, K., Stevens, B., Voigt, A., Roeckner, E., 2019. Mpi-m mpi-esm1.2-lr model output prepared for cmip6 scenariomip ssp585. doi:10.22033/ESGF/CMIP6.6705 http://cera-www.dkrz.de/WDCC/meta/CMIP6/CMIP6.ScenarioMIP.MPI-M.MPI-ESM1-2-LR.ssp585.

Wind systems https://manoa.hawaii.edu/exploringourfluidearth/physical/atmospheric-effects/wind-systems accessed: 2021-11-11.

Wu, J., Shi, Y., Xu, Y., 2020. Evaluation and projection of surface wind speed over China based on cmip6 gcms. NovJGR Atmos. 125 (22). https://doi.org/10.1029/2020jd033611 URL doi:10.1029/2020jd033611.

Xin, X., Wu, T., Shi, X., Zhang, F., Li, J., Chu, M., Liu, Q., Yan, J., Ma, Q., Wei, M., 2019. Bcc bcc-csm2mr model output prepared for cmip6 scenariomip. https://doi.org/10.22033/ESGF/CMIP6.1732 URL http://cera-www.dkrz.de/WDCC/meta/CMIP6/CMIP6.ScenarioMIP.BCC.BCC-CSM2-MR.

Yazdandoost, F., Moradian, S., Zakipour, M., Izadi, A., Bavandpour, M., 2020. Improving the precipitation forecasts of the North-American multi model ensemble (nmme) over sistan basin. J. Hydrol. 590, 125263. https://doi.org/10.1016/j.jhydrol.2020.125263 https://www.sciencedirect.com/science/article/pii/S002216942030723X.

Yu, Y., 2019. Cas fgoals-f3-l model output prepared for cmip6 scenariomip. https://doi.org/10.22033/ESGF/CMIP6.2046 URL http://cera-www.dkrz.de/WDCC/meta/CMIP6/CMIP6.ScenarioMIP.CAS.FGOALS-f3-L.

Yukimoto, S., Koshiro, T., Kawai, H., Oshima, N., Yoshida, K., Urakawa, S., Tsujino, H., Deushi, M., Tanaka, T., Hosaka, M., Yoshimura, H., Shindo, E., Mizuta, R., Ishii, M., Obata, A., Adachi, Y., 2019. Mri mri-esm2.0 model output prepared for cmip6 scenariomip. https://doi.org/10.22033/ESGF/CMIP6.638 URL http://cera-www.dkrz.de/WDCC/meta/CMIP6/CMIP6.ScenarioMIP.MRI.MRI-ESM2-0.

Zhang, S., Li, X., 2021. Future projections of offshore wind energy resources in China using cmip6 simulations and a deep learning-based downscaling method. Energy 217, 119321. https://doi.org/10.1016/j.energy.2020.119321 URL doi:10.1016/j.energy.2020.119321.

Energy in New Zealand, Tech. rep. Ministry of Business, Innovation and Employment.